AD-A150 087 IMPROVEMENT OF VHF(MB) MODEL(U) SCIENCE APPLICATIONS INTERNATIONAL CORP LA JOLLA CA D SACHS 12 NOV 84 SAIC-84/1634 N00339-81-C-0654 1/1

UNCLASSIFIED F/G 17/2.1 NL

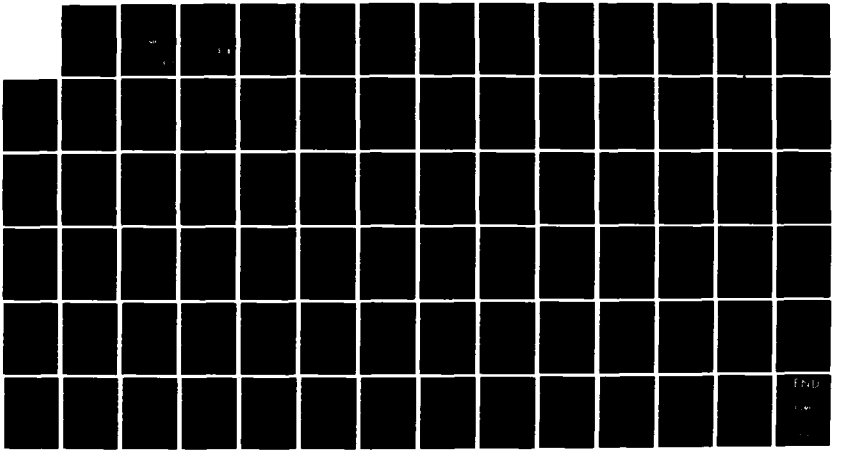

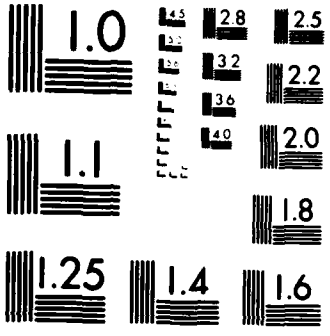

(2)

IMPROVEMENT OF VHF(MB) MODEL

SAIC™

Science Applications International Corporation

UNCLASSIFIED

SECURITY CLASSIFICATION OF THIS PAGE (When Data Entered)

REPORT DOCUMENTATION PAGE		READ INSTRUCTIONS BEFORE COMPLETING FORM
1. REPORT NUMBER	2. GOVT ACCESSION NO. AD-A150 087	3. RECIPIENT'S CATALOG NUMBER
4. TITLE (and Subtitle) IMPROVEMENT OF VHF(MB) MODEL		5. TYPE OF REPORT & PERIOD COVERED Engineering Report
		6. PERFORMING ORG. REPORT NUMBER SAIC 84/1634
7. AUTHOR(s) David Sachs		8. CONTRACT OR GRANT NUMBER(s) N00039-81-C-0654
9. PERFORMING ORGANIZATION NAME AND ADDRESS Science Applications International Corporation 1200 Prospect Street, P.O. Box 2351 La Jolla, California 92038		10. PROGRAM ELEMENT, PROJECT, TASK AREA & WORK UNIT NUMBERS
11. CONTROLLING OFFICE NAME AND ADDRESS Commander, Naval Electronic Systems Command Communications Systems Project Office Washington, D.C. 20363		12. REPORT DATE November 12, 1984
		13. NUMBER OF PAGES 80
14. MONITORING AGENCY NAME & ADDRESS(if different from Controlling Office)		15. SECURITY CLASS. (of this report) UNCLASSIFIED
		15a. DECLASSIFICATION/DOWNGRADING SCHEDULE N/A

16. DISTRIBUTION STATEMENT (of this Report)

This document has been approved for public release and sale; its distribution is unlimited.

17. DISTRIBUTION STATEMENT (of the abstract entered in Block 20, if different from Report)

Distribution limited to U.S. Government Organizations only, T&E. Other requests for this document must be referred to Commander, Naval Electronic Systems Command, Communications Systems Project Office, Washington, D.C. 20363. Attn: PDE 110-11.

18. SUPPLEMENTARY NOTES

19. KEY WORDS (Continue on reverse side if necessary and identify by block number)

Meteor-burst
Link Performance
Communications
Radio

20. ABSTRACT (Continue on reverse side if necessary and identify by block number)

The improvement of a VHF(MB) link performance model is described which consists of a program which evaluates signal reflecting properties and average rate of occurrence of meteor trails for elements of area of sky at 100 km altitude within the horizons for surface antennas.

Probabilities of message receipt are obtained by combining probabilities for each sky element. Both overdense and underdense meteor trails are considered.

DD FORM 1 JAN 73 1473 EDITION OF 1 NOV 65 IS OBSOLETE

UNCLASSIFIED

SECURITY CLASSIFICATION OF THIS PAGE (When Data Entered)

PREFACE

This report describes a VHF(MB) link performance model which was constructed in three phases. The most recent work, Phase III, is described in Section I of this report. This description assumes that the description of Phases I and II have been read. Phase II was described in a draft report which contained the description of Phase I in Appendix A of the report. The draft report is enclosed as Section II of this paper. Since the draft report of Phase III is enclosed as Section I of this paper, a chronological history of the model can be obtained by reading Appendix A, Section II and I in that order.

The first phase resulted in a description of meteor trail frequency and time dependence based on limited experimental data. Meteor trail frequency scaled with radiated power as if all trails were underdense. Formulas for probability of message receipt were developed for messages sent in broadcast mode and split in one to eight packets. The second phase consisted of the inclusion of overdense meteor trail phenomenology into the model. This inclusion indicated a degradation in performance at lower radiated power than predicted by the earlier model.

Phase III consisted of an examination of the model for agreement with experimental data and physics models for trail frequency and time dependence. It was decided that the original modeling of these quantities was too crude to account for the differences between the experimental situation where data was taken and the configuration of STRATSEC. Therefore a sky integration model was constructed which more accurately modeled the dependence of meteor trail frequency and time dependence on the experimental situation. The model was validated with some experimental data but further data comparison is needed. The new model was constructed for surface to surface links. Extension of the model to the case of one or both nodes at balloon altitude is needed for STRATSEC requirements.

SECTION I

SKY INTEGRATION MODEL

TABLE OF CONTENTS

LIST OF ILLUSTRATIONS

1. INTRODUCTION AND SUMMARY

A VHF(MB) link performance model was previously constructed[1] for application to STRATSEC. In this paper, we have reexamined the model for agreement with experimental data and physics models.

The first part of the reexamination dealt with the predictions of ground ranges between receivers wherein meteor trail reflection was not required for link connectivity. That is, the ground wave was adequate. The original model predicted ground wave adequate for ranges up to 200 km. We obtained and exercised a ground wave path loss computer program and found that 200 km was a reasonable bound for systems with acceptable path losses of 180-190 dB if the link was over the ocean or between antennas raised above poor ground. However, if antennas were lowered from 20m to 2m over poor ground, the ground ranges for acceptable loss was cut in half.

For the cases of surface to FFB and FFB to FFB links, the predictions of the original model were verified by the path loss computer program.

The second part of the reexamination dealt with the performance predictions of the meteor trail reflection phenomenon. This was based on two parameters, M_0 and τ, which are the rate of occurrence of reflecting meteor trails of a certain line density and the effective life time of the trail respectively.

The values of these parameters as a function of ground range between antennas were taken from the proposed model described in a final report by Meteor Communications Consultants, Inc. for the Naval Ocean Systems Center.[2] Recently, a report[3] submitted by John Ames of SRI International showed different values of these quantities than our model used. His numbers were based primarily on the work of A. E. Spezio[4] of the Naval Research Lab.

While studying the reasons for the discrepancies, we found that the use of single values of the parameters as representing the entire area where

meteor trails occur is too crude to effectively account for the differences between horizontal and vertical polarization and the parameter boundary where overdense trails are required.

We therefore constructed a computer program to sum contributions over the sky where useful meteor trails occur. In addition to providing better accuracy through the actual space dependence of τ, M_o and the overdense-underdense boundary, antenna patterns can be utilized for better reproduction of differing experimental situations for the purpose of validation.

The next section describes the computer program and how it combines with portions of the previous model described in Ref. 1 to become the new link performance model. Reference 1 is reproduced as Section II of this document. An understanding of the material in Ref. 1 is required to understand this section. The third section shows the new results and compares them with the predictions of the previous model and with some experimental data.

In summary, comparison of the previous model with experimental data and physics models shows that the model predicts over optimistic link performance.

We determined that this was due to the assumption of a single effective τ at path mid-range and the assumption that the overdense boundary depended only on the power factor. The model was modified to integrate each path of sky resulting in a more realistic link performance prediction for surface to surface links and the capability of including antenna patterns and polarization.

However, some uncertainty still exists for predicting performance with vertical polarization and wide beam antennas because of the lack of experimental data.

Further data is required for model calibration. In particlar, vertical polarization with azimuth-omnidirectional antennas over a series of ranges and powers would be useful.

The new model is applicable to surface to surface links only. Extension of the model to FFB nodes will require further analysis and further experimental data using FFBs or other elevated platforms.

2. THE NEW LINK PERFORMANCE MODEL

The new model uses the same formulas for probability and signal time behavior as the old model described in Ref. 1. Reference 1 is reproduced as Section II of this document. The major differences are in the fact that the new model performs the probability calculations for each portion of the sky where useful meteor trails occur and then combines the probabilities, and that the signal reflecting properties and time constant of the trail are more stringent than before.

For a given value of ground range between antennas, one quadrant of area of the sky at 100 km altitude is divided into squares 25 km on a side. This quadrant is one fourth the area bounded by 1000 km horizons of the two antennas. The following quantities are evaluated at the centers of the squares.

$\cos^2\Phi$, where Φ is half the scatter angle;

EM, a quantity related to the Eshleman-Manning[5] fraction of useful trails;

SOF, a quantity which contains the geometry-dependent part of the minimum trail line density for signal threshold.

These quantities are evaluated and stored for ground ranges from 200 to 1800 km in 200 km intervals. They are called by the new link performance model to evaluate probabilities of message receipt at one or more of the specified ground ranges for input values of the engineering parameters. The input parameters are unchanged from those required for the old model described in Ref. 1.

The old model stipulated an effective rate of occurrence of meteor trails with electron line density, q, of $q_o = 8.87 \cdot 10^{13}$ electrons/m. This

was about one every two minutes at mid ranges and less at longer and shorter ranges. This came from data from Ref. 2 which stated that a system which could tolerate 180 dB of path loss had a meteor rate ranging from one every minute to one every three minutes. We chose two every three minutes as a compromise. The reference stated the overdense-underdense boundary which corresponds to $q = q_0$ occurred for a system with half the power or any other change in engineering parameters which caused the tolerated path loss to be reduced to 177 dB. By underdense scaling this meant the test system described required a minimum line density $q = q_0/\sqrt{2}$ electrons/m. Therefore the meteor rate at the boundary was $M_0 = 2/(3 \text{ min}) \times 0.700 \approx 1/(2 \text{ min})$.

Unfortunately, the linking of meteor rate to the test system which had horizontal polarization and high gain antennas and applying that rate to a system which uses vertical polarization and antennas which are omnidirectional in azimuth causes the results to err on the optimistic side. This fact was not appreciated until the new model was built which demonstrated the difference in the two situations.

The new model obtains the meteor rate as follows. Eshleman and Manning[5] state the number of meteors per unit area per second entering the earth's atmosphere with line density q or higher is

$$N = C/q \text{ meteors/km}^2\text{/sec}$$

where $C \approx 1.6 \cdot 10^8$, a number we can use but also decrease to account for times of day or year when fewer are expected in the region of interest. Of these, a fraction, p, are oriented in such a way as to produce a reflection. The formula[5] is

$$p = \frac{50 \text{ km}}{3\pi D} \times EM$$

where the quantity evaluated over the sky,

$$EM = \frac{\left[3(\xi^2-\eta^2) - (1-\eta^2)\right]\left[(\xi^2-1)(\xi^2-\eta^2) - \xi^2h^2/D^2\right] - \eta^2(\xi^2-1)h^2/D^2}{(\xi^2-\eta^2)^2(\xi^2-1)\left[(\xi^2-1)(\xi^2-\eta^2) - \xi^2h^2/D^2\right]^{1/2}}$$

where h = meteor altitude = 100 km

D = 1/2 ground range, R ($R \equiv 2D$)

$\xi = (R_t + R_r)/R$

$\eta = (R_t - R_r)/R$

R_t, R_r = distances from antennas to point in sky.

Since there are four patches of sky with the same geometry, the total number of meteors/min of useful orientation for a $(25\ km)^2$ patch of the quadrant with a value of $q \geq q_o = (4pC/q_o)\ (25\ km)^2\ (60\ sec/min)$. Therefore $M_o = 1.8 \cdot 10^{-8} C\ (EM)/R$ meteors/min is the required rate.

The second quantity of concern is the meteor burst time constant,

$$\tau = \frac{\lambda^2 \sec^2 \Phi}{16\pi^2 d}\ (sec)$$

where λ = wave length (m)

d = diffusion coefficient (m^2/sec).

This is evaluated in the new model for each patch of sky. As suggested in Ref. 2, the old model used a single value of τ where Φ was obtained for a point at 100 km altitude midway between the antennas. Although this point has the largest value of $\sec^2 \Phi$ and hence τ of the sky, it was believed at the time that most meteor trails of importance occurred near that point. However, the new model shows many contributing meteor trails over a large region of sky which brings down the effective value of $\sec^2 \Phi$ and hence τ.

The new model also shows the difficulty of interpreting experimental

data on τ for the purpose of fixing the value of d. We have used d = $8m^2/s$ in the past. The appropriate value depends on the altitude of the trail. The diffusion coefficient varies from 0.5 at 80 km to 100 m^2/s at 100 km altitude. An experimental determination of τ by Keary and Wirth[6] show a two to one daily variation of τ which they attribute to higher velocity meteors in the early morning causing the trails to occur higher in the atmosphere where d is greater. Their experiment used horizontal polarization and Yagi antennas which lead to slightly higher values of effective τ than would obtain for vertical polarization and omnidirectional antennas. We illustrate this difference by using the code to calculate an effective τ by averaging over the sky weighted by EM/SOF which represents the relative number of useful underdense trails for a specific system. We show in Figure 1, the results of the calculation for a frequency of 47 MHz and d = $8m^2$/sec. The circles are the old midpoint calculation whose values are too high. The B's are the result of simulating an experiment by Boeing described in Section 3 which used horizontal polarizations and Yagi antennas. The x's result from vertical stub antennas which cover a larger region of sky. The dots are from Ames' report[3]. The Keary and Wirth data bar at 700 km range shows agreement at the low end but suggests that we could reduce d to $4m^2$/sec for early morning. One other data point from the COMET system (described in Section 3) at 1000 km falls directly on the B so we will stay with d = $8m^2$/sec.

The final quantity used for the probability calculations is S_o. This is the quantity defined in the old model as a required signal as determined by system parameters normalized to the overdense-underdense boundary at q_o. For $S_o < 1$, underdense trails sufficed. In the old model, S_o was matched to the data of Ref. 2. In the new model, S_o is taken directly from the radar transmission equation which includes the meteor trail scattering cross section.

$$\frac{P_t G_t G_r}{T_r} = \frac{16\pi^2 R_t R_r (R_t + R_r)\ (1 - \cos^2\beta \sin^2\Phi)}{\lambda^3 q^2 r_e^2 \sin^2\alpha\ g_t(\theta_t,\phi_t) g_r(\theta_r,\phi_r)} \quad .$$

The quantity on the left is the basic path loss (when in dB) that the system can tolerate to achieve the required threshold power, T_r. The radiated

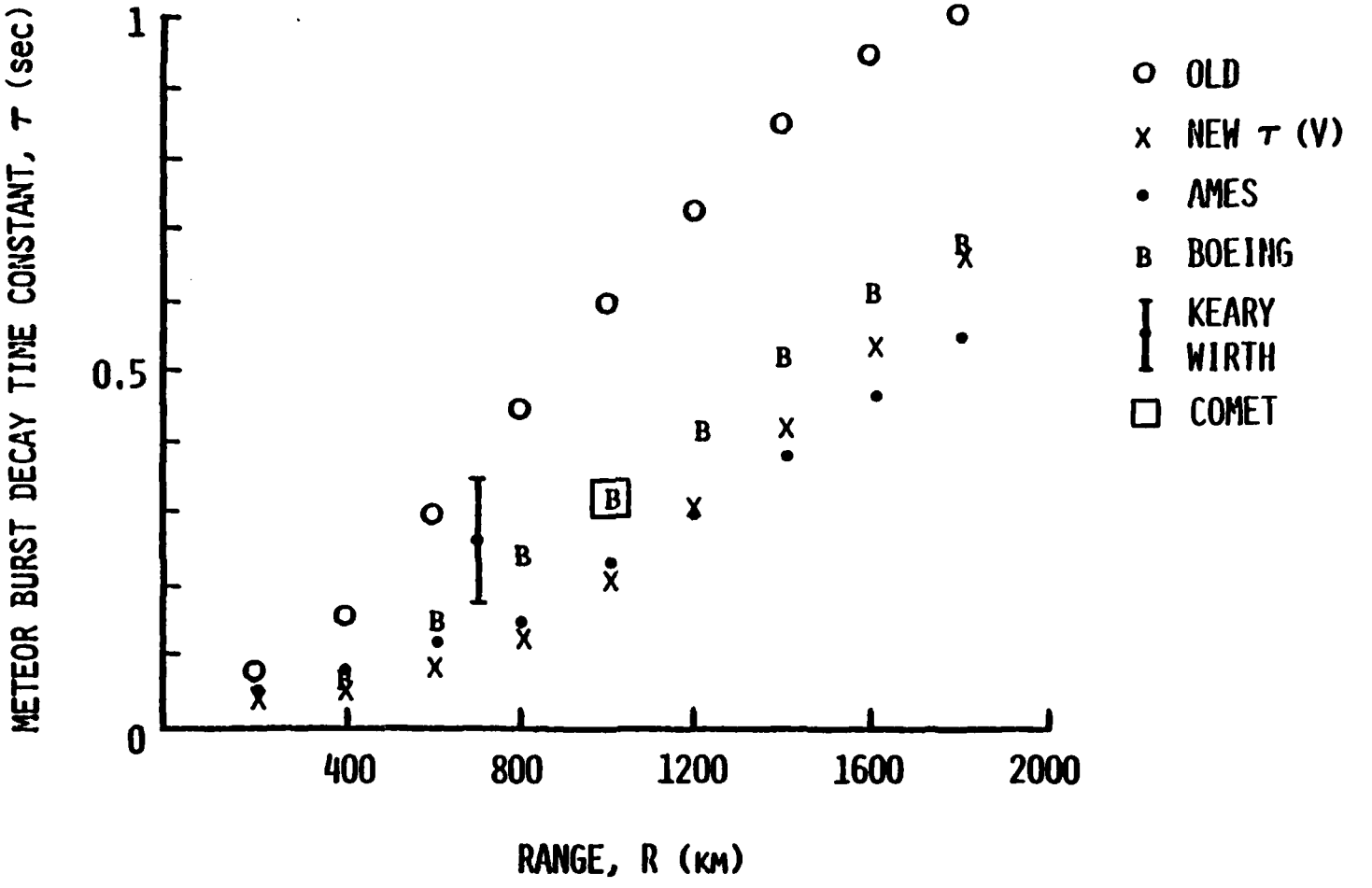

Figure 1. Time Constant Vs. Range.

power is P_t and G_t and G_r are the maximum gains of the antennas over an isotrope.

The quantity on the right is that loss in scattering from the properly oriented meteor trail of line density q where g_t and g_r are the normalized antenna gain patterns of transmitter and receiver. These are to be evaluated for the elevation and azimuth angles, θ and ϕ, to the point in the sky. The angle α is between the electric vector at the meteor trail and $\vec{R}_r$, the direction vector from meteor trail to receiver and β is the angle between the trail and the plane of $\vec{R}_t$ and $\vec{R}_r$.

We choose the value of S_o as the normalized line density required for the experimental and geometrical parameters involved.

$$S_o = \frac{q}{q_o} = 16\pi \sqrt{\frac{T_r}{P_t G_t G_r \lambda^3}}\, SOF(\beta)$$

where

$$SOF(\beta) = \sqrt{\frac{R_t R_r (R_t + R_r)(1 - \cos^2\beta \sin^2\Phi)}{\sin^2\alpha\; g_t(\theta_t,\phi_t) g_r(\theta_r,\phi_r)}}$$

by substitution from the transmission equation.

Since Eshleman and Manning[5] integrated over β to obtain their fraction of properly oriented trails, we must integrate over β to obtain the proper average for the probability calculations without knowing how to weight the values of β in the averaging process. The proper average is of the quantity $1/SOF(\beta)$ or

$$\frac{1}{\sqrt{1 - \cos^2\beta \sin^2\Phi}}$$

which, for trails uniformly distributed in β, has the average

$$\frac{2}{\pi} K (\sin \Phi)$$

where K is the complete elliptic integral of the first kind. We choose instead the simpler quantity

$$\frac{2}{1 + \cos \Phi}$$

which is close to the average but smaller for large Φ making the model conservative. The true weighting over β is unknown without redoing the work of Eshleman and Manning. We therefore use

$$SOF = \frac{(1 + \cos \phi)}{2 \sin \alpha} \sqrt{\frac{R_t R_r (R_t + R_r)}{g(\theta_t,\phi_t) g(\theta_r,\phi_r)}} .$$

For vertical stick antennas,

$$g(\theta,\phi) = \cos^2 \theta$$

and the maximum gain over an isotrope, G = 3/2.

Finally, the quantities S_o, M_o and τ as specified are used as described in Ref. 1 to calculate the probability of not receiving a signal of required value S_o and time length Δt (no useful meteor bursts) assuming no useful meteor bursts occurred prior to a time T before the signal was sent. This is done for each part of the sky and their product is then the appropriately combined probability for the entire sky. This is used to obtain the probability of message receipt as described in Ref. 1.

3. PREDICTIONS AND DATA COMPARISON

The new model has the capability of being adjusted to reproduce different experimental situations. We illustrate this by comparing it with some performance measurements taken by Boeing described in NOSC TR138[7]. Data was taken for two paths of 800 and 1600 km ground range. A probe signal was continuously sent from a master to a remote station. If a meteor trail occurred of sufficient strength for the remote station to detect the probe signal, the remote station sent a small block of data to the master station over the same trail. The performance data was in the form of probability of success vs. waiting time. This data was averaged over a two week period for six 4 hour time blocks to show the daily variation of meteor rate.

The allowable path loss for the probe signal was 191 dB. The allowable path loss for the response signal was 199.7 dB. The probe signal required a stronger meteor trail by 8.7 dB primarily because of the noisy remote receiver.

This means the occurrence of a meteor trail strong enough for the remote receiver to detect the probe signal will allow the remote station to send the short data block (which required $\Delta t = 0.156$ seconds) on the same trail whose scattering cross section would have diminished by a factor $e^{-2\ \Delta t/\tau}$.

For 8.7 dB, $\tau \geq 0.156$ seconds is sufficient for the correct message receipt to be determined solely by the probe path loss of 191 dB. From Figure 1, the Boeing values of τ are greater than 0.2 sec.

In the expression for SOF, on page 10 we alter the calculation of sin α to account for horizontal polarization and use the experimental values of $G_t = 20$ (13 dB) and $G_r = 6.3$ (8 dB) in an approximate expression for the normalized gain pattern

$$e^{-G(\theta^2 + \phi^2)/4}$$

The first data check on the new model is the ratio of average waiting time for the two ranges 800 and 1600 km. The data show the waiting time ratio to be about 2 (the longer range has the larger waiting time). This is in agreement with the model for a 191 dB system but not lower path loss systems. The old model also showed a factor of 2 but had no dependence of the factor on allowable path loss. Since the output can be put in the form of useful meteor rate M through the formula for probability of success vs. waiting time t,

$$P = 1 - e^{-Mt} \tag{1}$$

we match their curves of P vs. t to the formula and obtain the following values of M:

Time of Day	0-4	4-8	8-12	12-16	16-20	20-24
M	1.6	2.3	1.7	1.0	0.75	0.6
$C(\times 10^8)$	0.9	1.3	0.94	0.55	0.4	0.33

The third row contains the corresponding values of C by which the model would predict the values of M. We recall that C was associated with the overall rate of meteors entering the earth's atmosphere which Eshleman and Manning[5] estimated as $1.6 \cdot 10^8$. The experimentally determined values of C are slightly lower but very close. The old model would have predicted

$$M = M_o \, 10^{.05\,(11\ dB)} = 2/3\ (3.55) = 2.4$$

which is too high.

The experiment was in June and showed a daily variation of meteor rate of 4 to 1. July and August are supposed to have the highest rates and February, the lowest. The ratio of summer/winter rates is not precise, ranging from 1.4 in Ref. 2 to 5 in Ref. 7.

In order to demonstrate the difference between the old and new model, we reproduce a curve of probability of correct message receipt vs. power factor $P_t G_t G_r$ from Figure 14 of Ref. 1 in Figure 2. Using the identical parameters in the new model for short stub vertical antennas and a value of $C = 1.4\ 10^8$ as the incident meteor rate at the best time of day and year we obtain the curves shown in Figure 3. The new model shows much higher power factors required throughout. Some of the difference is due to the more conservative values of M_o and τ, but a major difference is the new method of treating the underdense/overdense boundary. The old model put the boundary at a 500 watt power factor. This is the "waterfall" region of Figure 2. The new model shows overdense bursts to be required everywhere for a 1400 km range until the power factor becomes greater than 2500 watts. We illustrate this point by contour plots of S_o vs. sky position for three ground ranges of 600, 1000 and 1400 km in Figures 4, 5 and 6 for a 180 dB system at 47 MHz. In the examples of Figures 2 and 3 this corresponds to a power factor of 1000 watts. The coordinates are distances from the midpoint in km. The abscissa is along the line between antennas. In Figures 4 and 5, the region above one antenna is shown to require high values of S_o due to polarization losses. This doesn't happen for horizontal polarization. The overdense boundary is at $S_o = 1$. Since S_o scales as the square root of power, at 4000 watts the boundary would be at the contour marked $S_o = 2$. According to Figure 3, this power increase is sufficient to increase all probabilities to greater than 0.96.

We have used the best meteor rate for a comparison with the old model and found the old model too optimistic. We will choose a worst rate as one fourth the best to typify a bad time of day in a good month or vice versa. The results are shown in Figure 7. Now much higher powers are required for the same broadcast time.

Since all results are functions of the product of overall meteor rate, C, and broadcast time, t. We can reproduce Figure 3 for the worst rate by increasing broadcast time to 40 min.

Finally, we illustrate the best case code predictions for a single packet of 512 bits at a data rate of 4000 bps at 47 MHz for the vertical stub

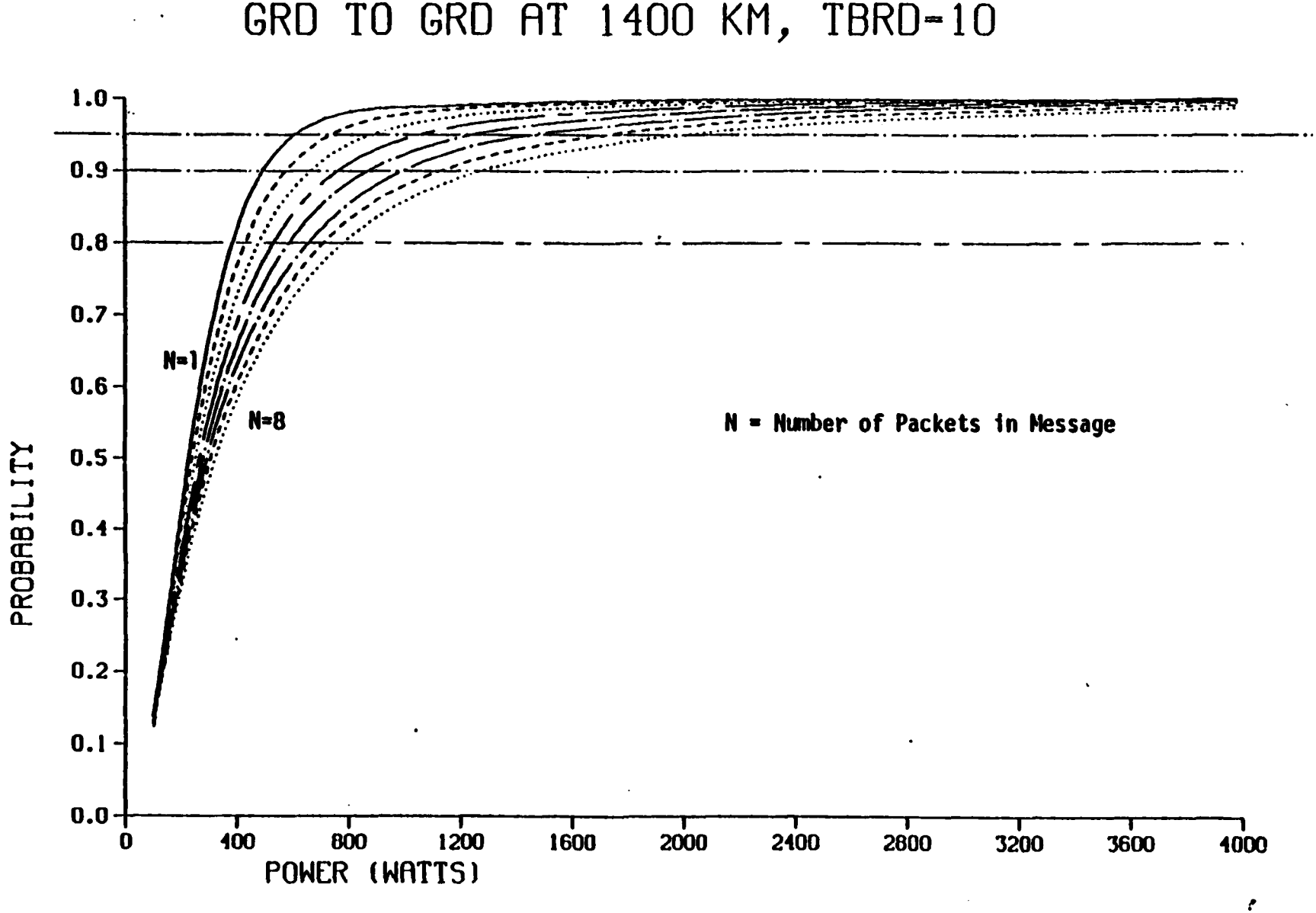

Figure 2. Probability of Correct Message Receipt Vs. Power Factor $P_t G_t G_r$.

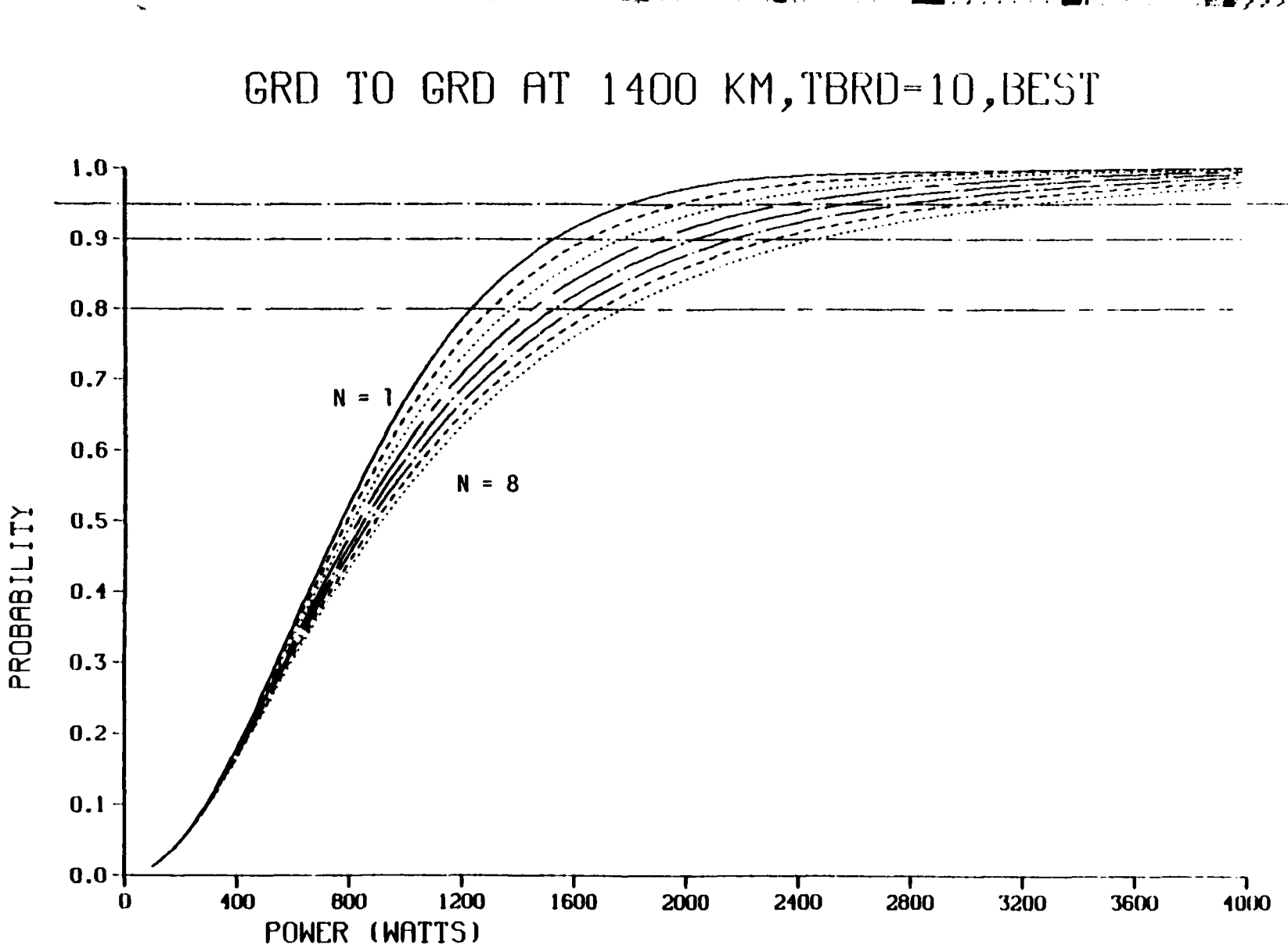

Figure 3. Probability of Correct Message Receipt Vs. Power Factor $P_t G_t G_r$; New Model, Best.

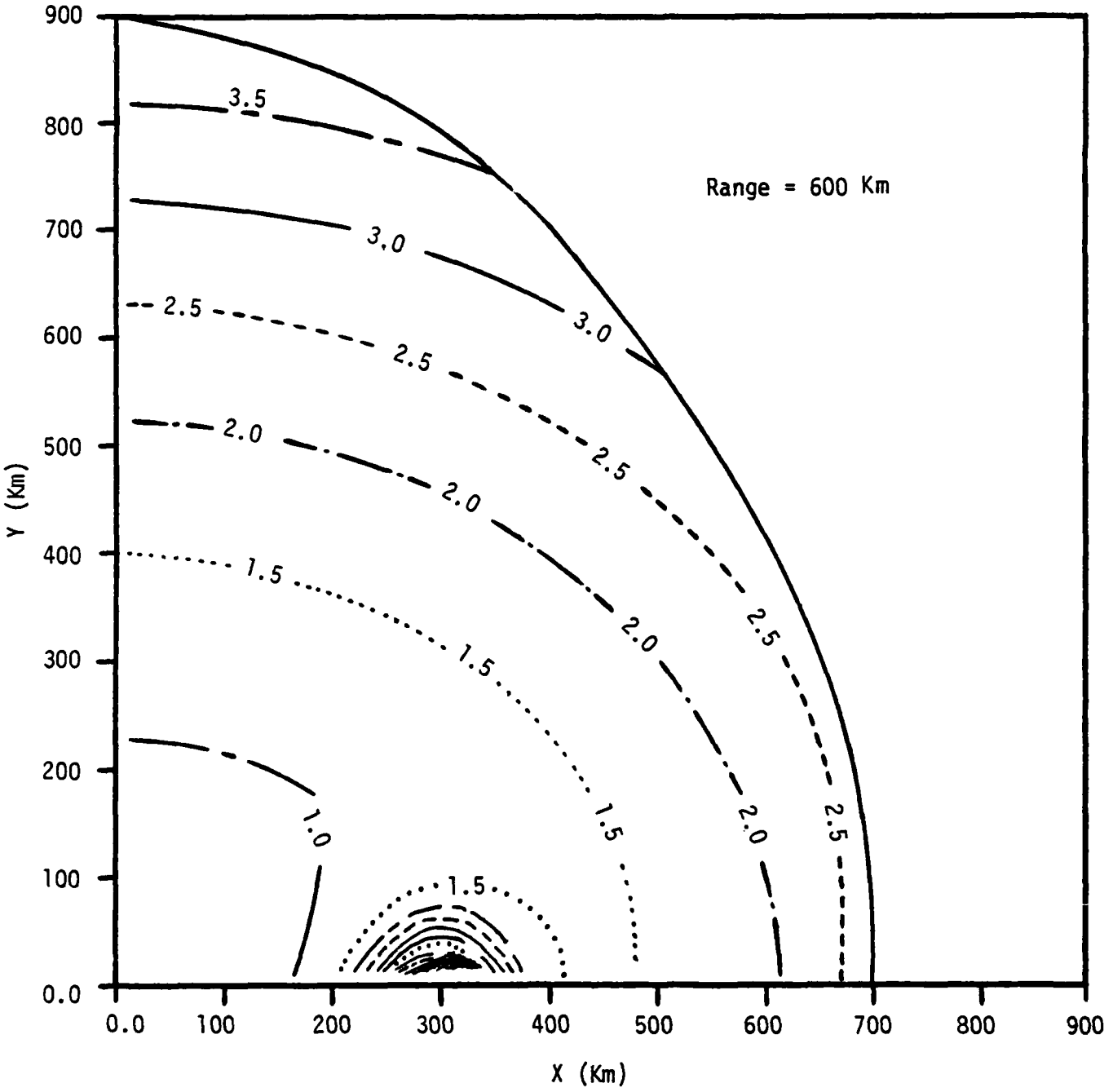

Figure 4. S_o Contours for Range = 600 Km, Vertical Stubs.

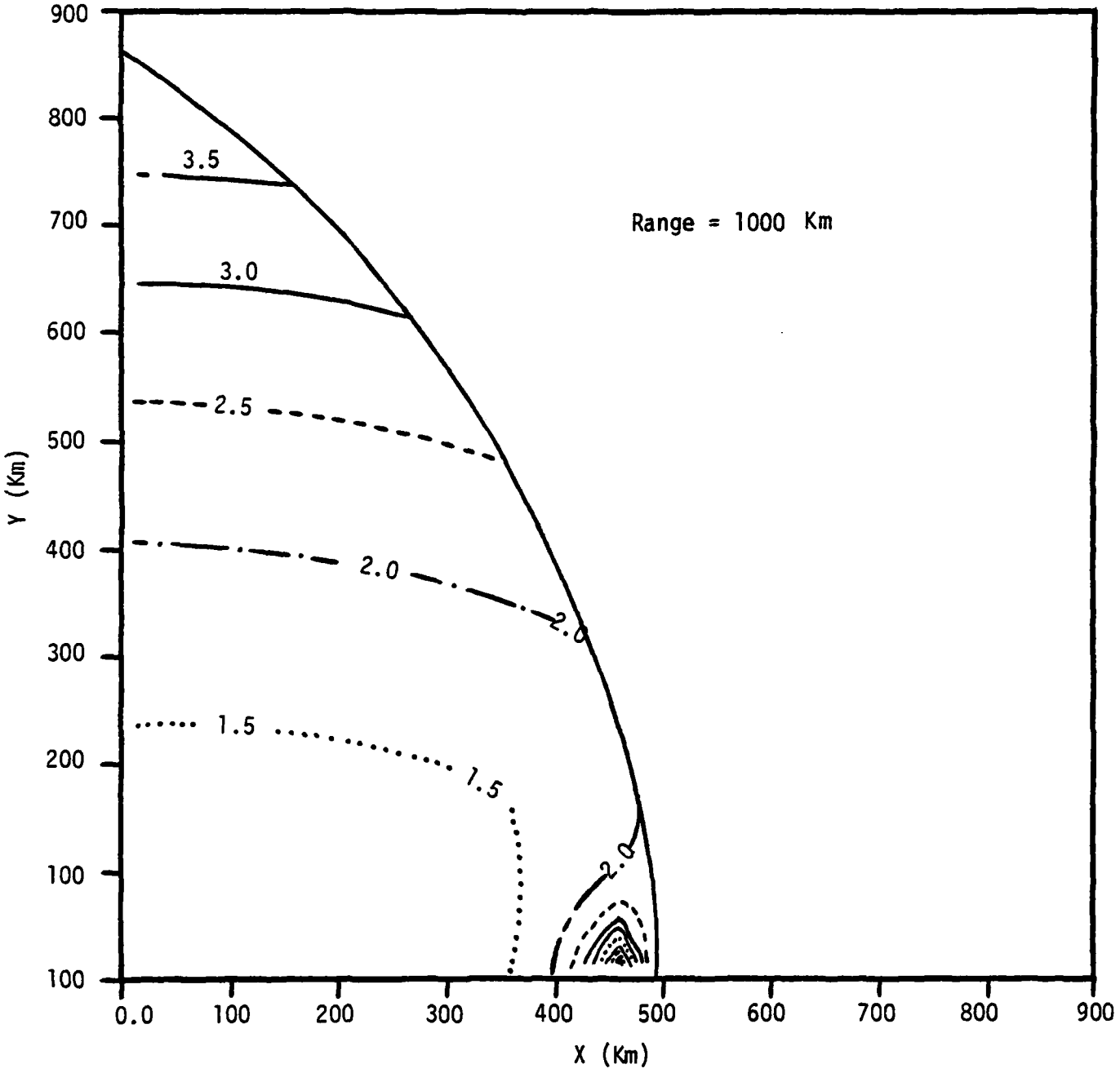

Figure 5. S_o Contours for Range = 1000 Km, Vertical Stubs.

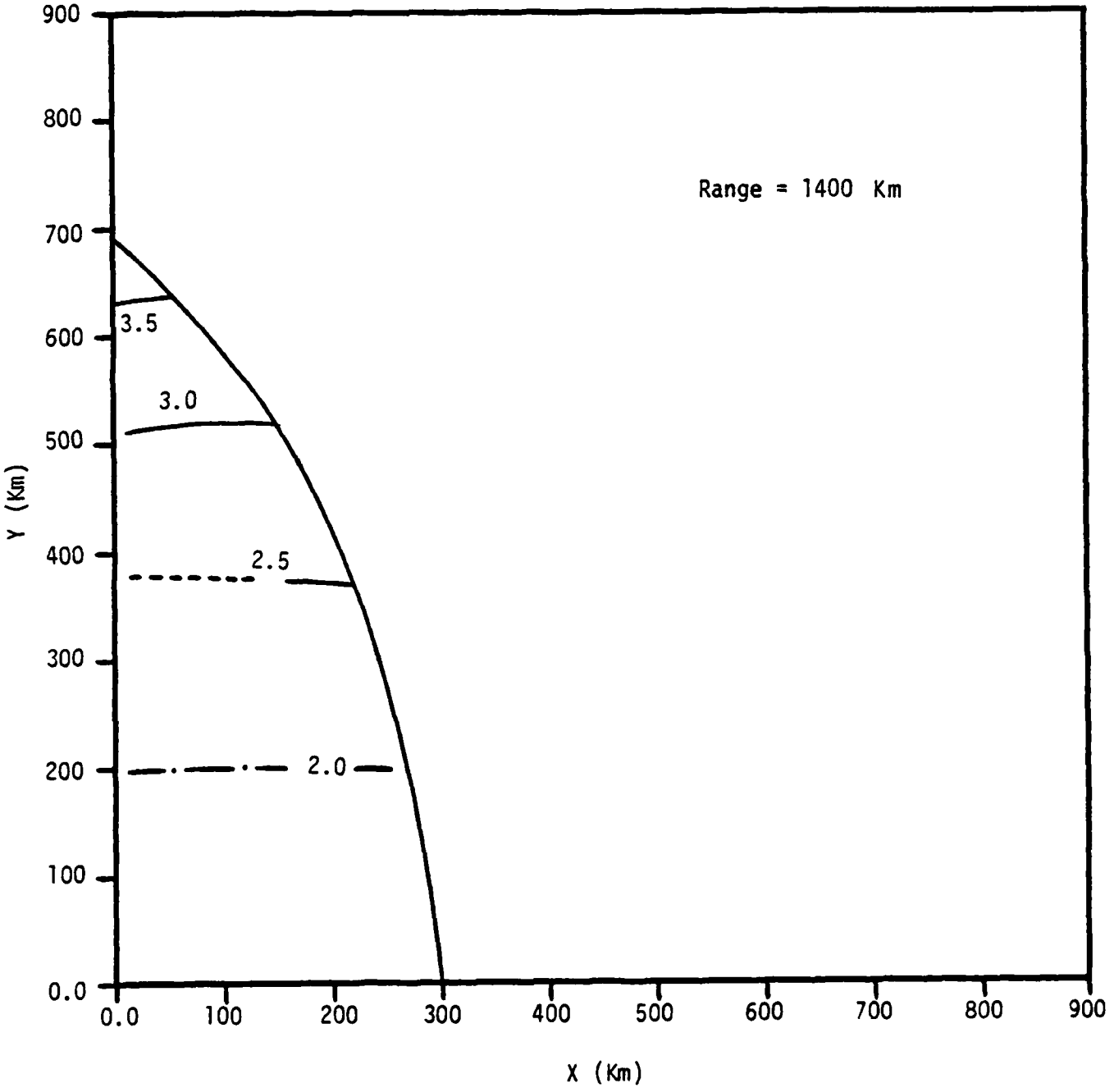

Figure 6. S_o Contours for Range = 1400 Km, Vertical Stubs.

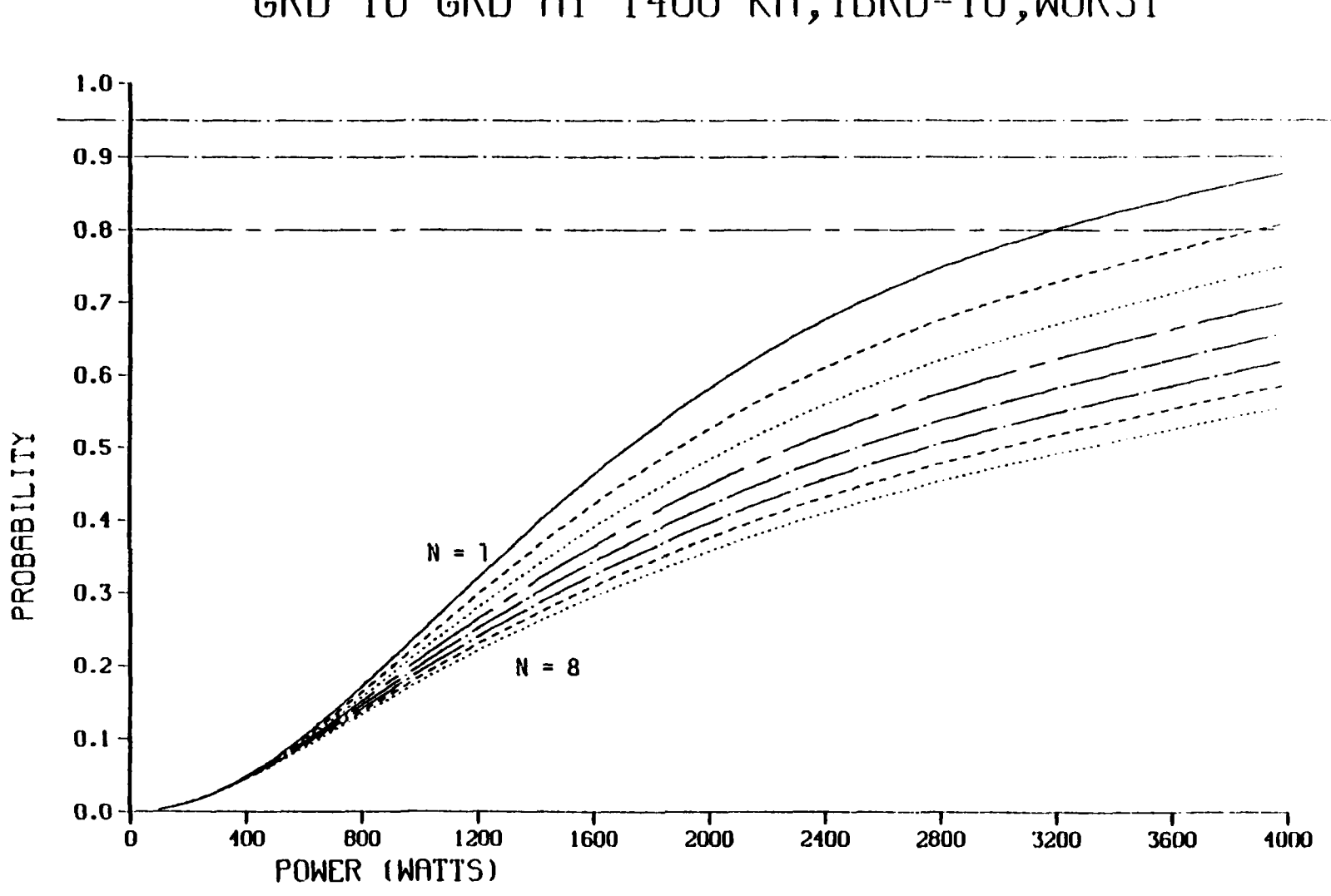

Figure 7. Probability of Correct Message Receipt Vs. Power Factor $P_t G_t G_r$; New model, Worst.

case in the form M_v vs. range in Figure 8. The various curves show the performance gain obtained by increasing the allowable path loss L_B. For the case considered, an L_B of 180 dB translates to a power factor of $P_t G_t G_r$ = 1000 watts. Therefore 190 dB corresponds to 10,000 watts. These curves can be used to obtain the probability of message receipt for a broadcast time t by expression (1) on page 12. For example at 1400 km, the 180 dB curve shows M_v = 0.112/min. Therefore a broadcast time of 10 min produces a probability $p = 1-e^{-1.12} = 0.67$ as seen on Figure 3. To obtain the worst case, we divide M_v by 4 to obtain $p = 1-e^{-0.28} = 0.244$ as shown on Figure 7.

The curves of Figure 8 indicate that higher power factors than previously thought are needed to overcome the overdense effects at the longer ranges.

Although the results presented here are pessimistic compared to the old model, they should get better at long ranges by the use of antennas with better gain patterns than the stubs used here for illustration. Also, the effect of one or more elevated nodes has not been analyzed. The old model assumed the effect to be the same maximum meteor rate at midrange with a longer extent until long range cut off. The mid range could actually turn out to have a higher meteor rate because of the longer horizon and the fact that portions of the sky far from the midpoint are useful for vertical polarization.

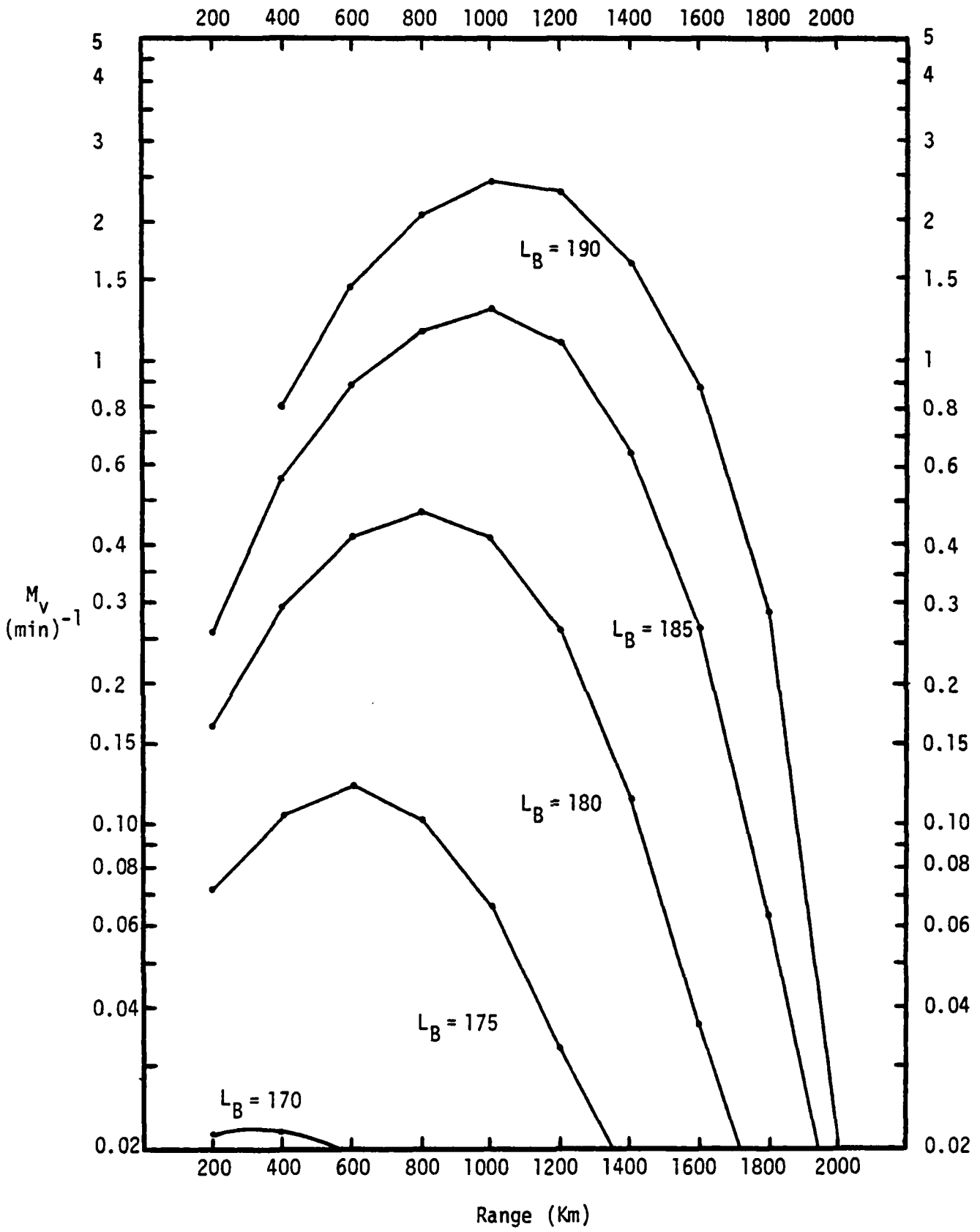

Figure 8. Meteor Rate Vs. Range, BEST, Vertical Stub.

REFERENCES

1. "Improvement of VHF(MB) Model. I. Overdense Meteor Trail Model," for Naval Electronic Systems Command, Contract N00039-81-C-0654, October 7, 1983.

2. Final Report, "Analysis of Meteor Burst Communications for Navy Strategic Applications," for Naval Ocean Systems Center, Contract No. N66001-79-C-0460, February 4, 1980.

3. Ames, John W., "Stratsec Transportable Shore Node - Link Design for the VHF Meteor-Burst Broadcast Relay Element," for Naval Electronic Systems Command, Contract No. N00039-81-C-0086, January 1984.

4. Spezio, Anthony E., "Meteor-Burst Communication Systems: Analysis and Synthesis," NRL Report 8286, Naval Research Laboratory, Washington, D.C., December 28, 1978.

5. Eshleman, Von R., and Laurence A. Manning, "Radio Communication by Scattering from Meteoric Ionization," Proceedings of the IRE, March 1954, p. 530.

6. Keary, T. J. and J. H. Wirth, "Statistical Characteristics of Forward-Scattered Radio Echoes from Meteor Trails," in "Electromgnetic Wave Propagation," Academic Press, New York, N. Y. p. 277; 1960.

7. Heritage, J. L., J. E. Bickel and C. P. Kugel, "Meteor Burst Communication in Minimum Essential Emergency Communication Network (MEECN)" for the Defense Communications Agency (DCA), Command and Control Technical Center (CCTC), August 16, 1977.

SECTION II

OVERDENSE METEOR TRAIL MODEL

TABLE OF CONTENTS

LIST OF ILLUSTRATIONS

LIST OF TABLES

1. INTRODUCTION

A VHF(MB) link performance model was previously constructed[1] for application to STRATSEC based on the physics of underdense reflection of radio signals by meteor trails. This report describes the improvement of that model by the inclusion of overdense reflection characteristics. The model improvement removes erroneous high predictions of performance by non existent underdense trails which the model required for low power levels.

All underdense models assume the signal reflected by the trail to be proportional to q, the electron line density.

$$S = r_e q e^{-t/\tau} \tag{1}$$

where $r_e = 2.8 \cdot 10^{-15}$ m = classical electron radius and τ is the trail time constant. The overdense variation of the signal is[2]

$$S = \left[\frac{t}{(4\pi)^2\tau} \ln\left(\frac{4r_e q\tau}{t}\right)\right]^{1/4}$$

which has a maximum value of

$$S_m = \left(\frac{r_e q}{4\pi^2 e}\right)^{1/4}$$

and drops to zero at $t = 4r_e q\tau$ when the trail is completely underdense.

Any meteor trail can be considered to have an overdense core and an underdense outer shell at early time with the overdense core shrinking to zero at $t = 4r_e q\tau$. For small values of $4r_e q$, the overdense signal is short lived and the dominant behavior is given by Eq. (1). The previous model assumed this variation for all values of q and t.

For large values of $4r_e q$, however, the overdense core is the actual reflection mechanism until $t = 4r_e q\tau > \tau$ after which some residual underdense signal is possible. In this case the overdense signal maximum value, S_m, is less than $r_e q$ and the real signal value is smaller than the underdense-only theory prediction.

This impacts the link performance model in the following way. The output of the model is the probability of receiving a message by meteor burst reflections which depends on the quantity M, the average rate of useful meteor trails. Since the frequency of trails is inversely proportional to the square of their line density, the higher a line density required to reflect a signal, the lower the value of M.

The original model obtained the value of M by scaling from data obtained from underdense trails.[3] From that data, M_{oo}, the average rate of useful meteor trails was determined. Reference 3 outlined a method of scaling from their test system to any other system operating at the same optimum ground ranges. For a required receiver threshold T_r(watts) which sets the required received signal amplitude $\sqrt{T_r}$, and given values of transmitter gain, G_t, above an isotrope, transmitter radiated power, P_t; receiver gain, G_r, above an isotrope and wavelength, λ, the required value of signal reflected by the trail ($\propto \sqrt{\text{cross-section}}$) is proportional to

$$\sqrt{\frac{T_r}{P_t G_t G_r \lambda^3}} \quad .$$

For the test system[3],

$$\lambda = 6.383 \text{ m}$$

and

$$\frac{P_t G_t G_r}{T_r} = 10^{18} \quad .$$

Therefore, the required value of signal for any other system scales as

$$S_{oo} = \sqrt{\frac{T_r \times 10^{18}}{P_t G_r G_t} \left(\frac{6.383}{\lambda}\right)^3}$$

For underdense bursts, $S_{oo} \propto q$ and since the average rate of meteors with line density q or higher is proportional to 1/q, the scaling for underdense bursts is

$$M = M_{oo}/S_{oo} \quad .$$

For a system with a large value of S_{oo} where the corresponding value of q is so large that only the overdense reflection is operative, the signal is $\propto q^{\frac{1}{4}}$ and not q. In this case the required q scales as S_{oo}^4 and the rate of useful meteors is $M \propto S_{oo}^{-4}$, which is lower than the underdense scaling. With lower values of M, the probability of message receipt will be lower than predicted by the underdense scaling.

The next section describes the analysis of overdense theory and the improved link performance model. The third section shows the new results and compares them with the predictions of the old model. The description of the old model in Ref. 1 is included as Appendix A and Appendix B describes the implementation of the new model as a computer program.

2. ANALYSIS

In this section, the transition point for underdense-overdense reflections is obtained and the method of describing overdense signals and the impact on probability calculations is described.

Reference 3 described the transition point to be at

$$M/M_{oo} \approx 0.7 \quad .$$

This value agrees with our conjecture in our description of overdense effects in reference 1 that the transition would occur at $S_{oo} \approx \sqrt{2}$.

In our previous engineering model[1], the value of M_{oo} was constant over most of the range with a linear fall off at large range due to shadowing of the useful area of sky by the curvature of the earth. Since this shadowing has nothing to do with required signal strength, the overdense scaling should apply to the long-range diminished M_{oo} also.

In addition, there was a slight fall off at short ranges for surface to surface links only. This fall off was attributed to geometric and polarization effects. This means the required signal strength is greater at the short ranges and the scaling should be different. We have insufficient information as to all the reasons for the short range fall-off to know how to change the scaling. Until we obtain that information we will apply the overdense scaling to the short-range diminished M_{oo} also.

We define a dimensionless q which is unity at the transition point $S_{oo} = \sqrt{2}$. We scale to the transition point by defining $M_o = M_{oo}/\sqrt{2}$, $S_o = S_{oo}/\sqrt{2}$ so that the average rate of meteors with line density q or higher is $M = M_o/q$ and the signal reflected by a trail of line density q has a maximum

$$S(q) = q \qquad q<1$$

$$S(q) = q^{\frac{1}{4}} \qquad q>1 \quad .$$

The required signal as determined by the system parameters is S_o. For $S_o \ll 1$, underdense meteor trails suffice. For $S_o \geq 1$, overdense meteor trails are required. If S_o is near and below unity, overdense trails may still be required.

Since we wish an entire message or packet of length Δt to be reflected by a single trail, the required reflecting signal must be greater than $S_o e^{\Delta t/\tau}$ since an underdense trail has reflecting signal time dependence

$$S = qe^{-t/\tau} \quad .$$

The overdense signal has a complicated time dependence which is obtained from an approximate theoretical treatment. The important characteristics are its maximum and the time at which it goes underdense which is proportional to q.

Examples of signals from overdense bursts are shown in Figure 1, an extract from a chart recording obtained at a receiving site over a 60 mile path using a 10 watt CW transmitter.[4] The large seven-second signal and the final two are overdense. The many small and one larger signal following the seven second signal are underdense. The fading in the large signal makes it less useful than one would predict from its average envelope value. It appears that short signals, $\Delta t < 1$ sec have a high probability of transmission if the required strength is half the envelope value. The small overdense signals do not exhibit this fading and in fact appear closer to the exponential time behavior of underdense signals.

In order to be conservative and for ease of computation, we will treat the overdense signals as if they also had an exponential time decay but with a longer time constant associated with the overdense period.

The transition will be smooth if we choose the time behavior of the overdense signal as

$$S = \begin{cases} q^{\frac{1}{4}} e^{-t/\tau q} & t \leq \tau q \\ q^{\frac{1}{4}} e^{q-1} e^{-t/\tau} & t > \tau q \end{cases}$$

which drops to 1/e of its initial value at the end of the overdense period and then diminishes further as an underdense trail.

We now outline the procedure for the determination of the probabilities of message receipt. As shown in the original model description[1], all possible probabilities of interest are obtainable from the following probability:

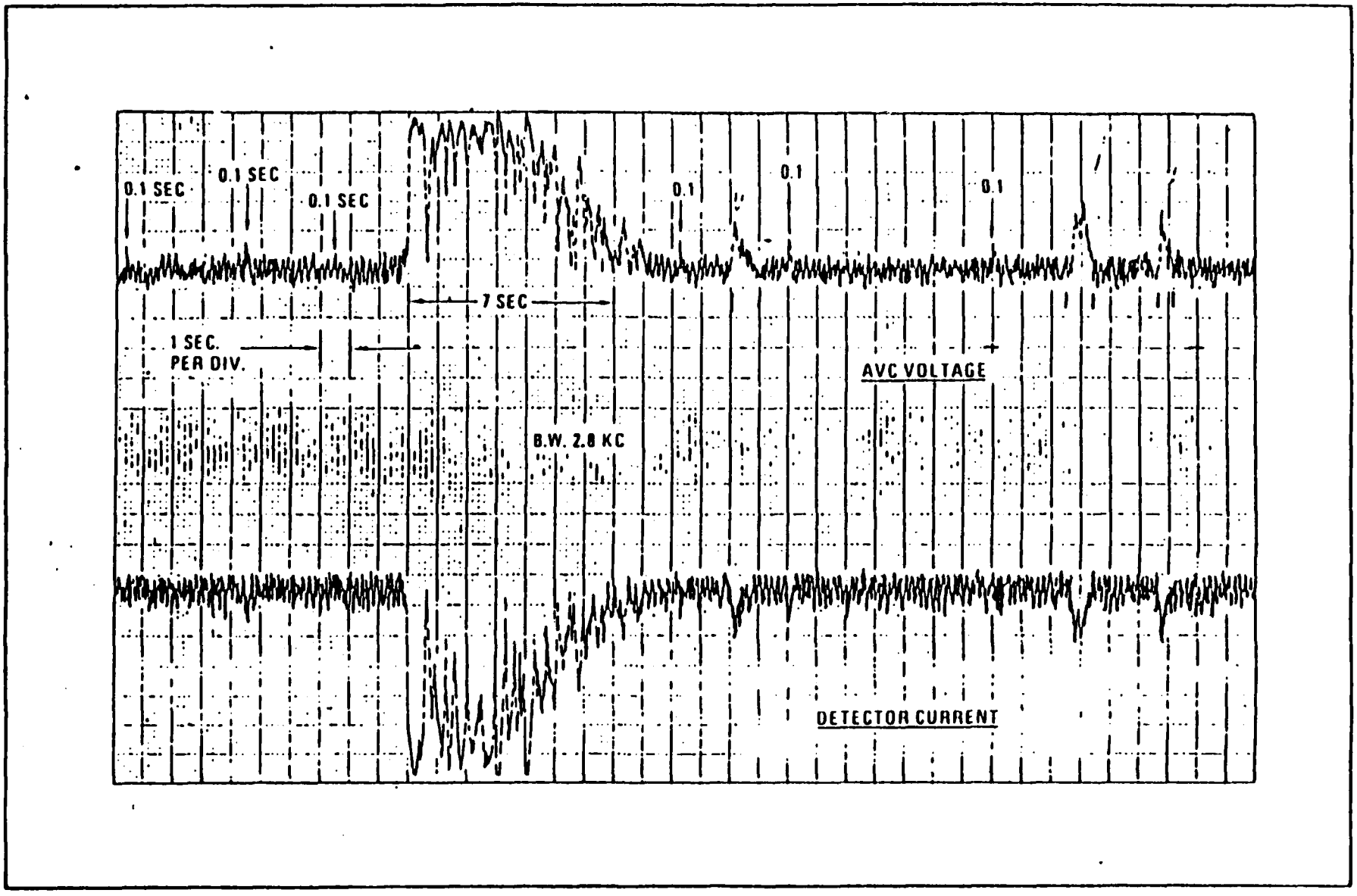

Figure 1. Extract from Chart Recording at Receiving Station Showing Overdense and Underdense Type Signals.

$\bar{P}(S_o,\Delta t,T)$ is the probability of <u>not</u> receiving a signal of required value S_o and time length Δt (no useful meteor bursts) assuming no useful meteor bursts occurred <u>prior</u> to a time T before the signal was sent.

Because of the change in the assumed time-dependence of the signal strength depending on whether the meteor trail is overdense or underdense, several cases need to be considered in order to calculate the relevant probabilities. These cases depend on whether the amplitude of a reflected signal decays as $e^{-t/\tau}$ (an underdense trail), $e^{-t/q\tau}$ (an overdense trail), or changes character during the relevant time. Probabilities for the different cases are described below. The situation is diagramed in Figure 2 for the underdense case where $S_o e^{\Delta t/\tau} << 1$.

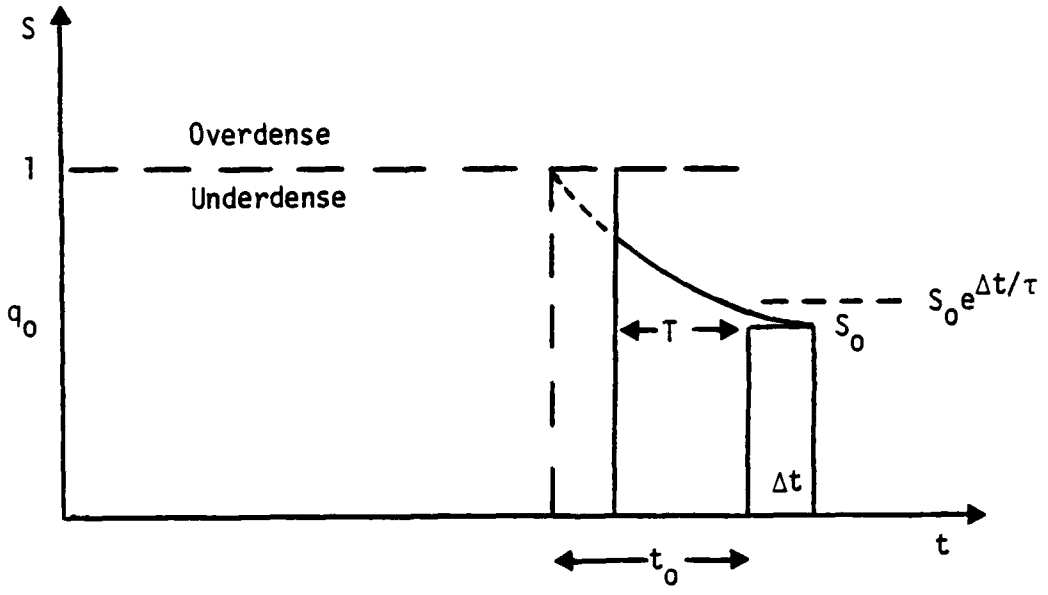

Figure 2. $T < t_o$, Underdense Only.

Because of the time dependence of the reflected signal, the minimum q required for sufficiently reflecting the signal depends on the time frame prior to the time the signal was sent. The time t_o corresponds to the prior time which requires a minimum value of q=1, the transition value,

$$t_o = -\tau\, \ell n(S_o) - \Delta t, \text{ a positive number} \quad .$$

The fact that $T < t_o$ means we are not concerned with overdense bursts since we are given that no useful bursts occurred prior to T before the signal. In this case

the formula for the probability is that derived in Ref. 1. We will rederive it here to illustrate the procedure.

For a meteor with line density in an interval dq about q, the average rate is $(M_o dq/q^2)$ and the prior time interval within which this meteor is useful is

$$t(q) = \tau \, \ell n \, (q/q_o)$$

where

$$q_o = S_o e^{\Delta t/\tau}$$

is the minimum useful value of q. For the given time and the given average rate, the probability that a meteor of that type does <u>not</u> occur in that time is

$$\overline{P}(q) = e^{-\frac{M_o dq}{q^2} t(q)} .$$

We assume the occurrence of a meteor of one value of q to be independent of the occurrence of a meteor with another value of q and multiply the probabilities of nonoccurrence of the various types.

For values of $q \geq q_M \equiv q_o e^{T/\tau}$ such that $t(q) \geq T$, the probability of nonoccurrence is

$$\overline{P}(q) = e^{-\frac{M_o dq}{q^2} T}$$

since none occurred prior to T before the signal.

The total probability of nonoccurrence

$$\overline{P}_u(S_o,\Delta t,T) = e^{-\int_{q_o}^{q_M} \frac{M_o dq}{q^2} \tau \ell n \, (q/q_o)} \; e^{-\int_{q_M}^{\infty} \frac{M_o dq}{q^2} T}$$

$$= e^{-\frac{M_o \tau}{q_o}(1-e^{-T/\tau})}$$

as derived previously in Ref. 1.

The fact that we have integrated beyond q=1 means that we have included overdense bursts in the probability calculation. They have been correctly included since all we need to know is that an overdense burst occurring within time T of the signal will be useful and that is automatically true for $T \leq t_o$.

The underdense reflection situation for $T > t_o$ is diagramed in Figure 3.

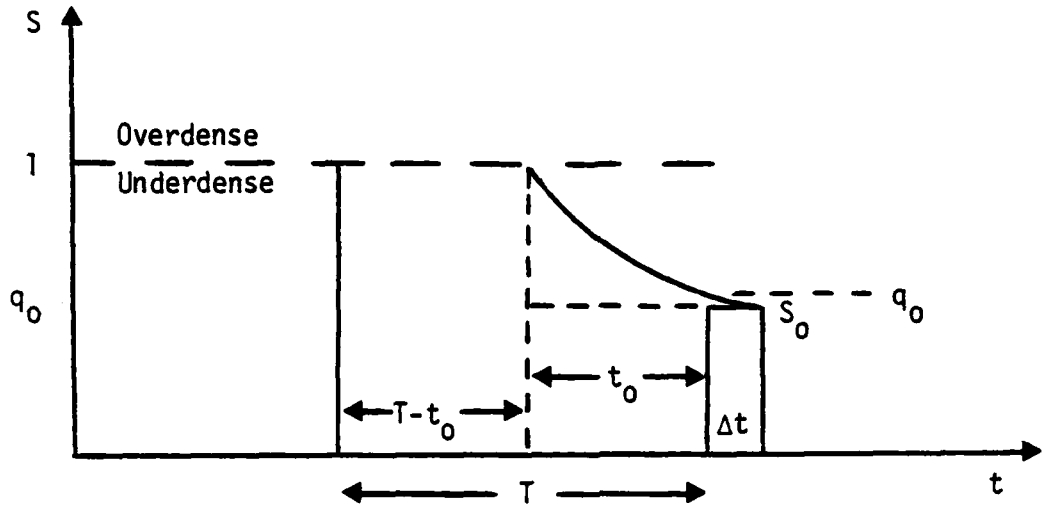

Figure 3. $T > t_o$, Underdense, Plus Overdense.

For this case, the probability of no useful meteor is the product of the probability of no useful meteor in time t_o (which is an underdense situation) and the probability of no useful meteor of $q > 1$ in the remaining time $(T-t_o)$. A glance at the figure shows the latter probability to be identical to the probability that would be calculated in an overdense case for prior time $(T-t_o)$ and a signal of length $\Delta t+t_o$. Denoting $\overline{P}_o$ for the calculated probabilities where $q_o \geq 1$ (overdense case), we have $\overline{P} = \overline{P_u}(S_o,\Delta t,t_o)\ \overline{P}_o(S_o,\Delta t+t_o,\ T-t_o)$.

In the general case of overdense trails, we will have to include the probability of occurrence of meteors with $q \geq q_1$ where $q_1 \geq 1$ is the smallest relevant meteor trail strength. (In the above case we know $q_1 = 1$.) For any $q \geq 1$, the signal form

$$S = q^{\frac{1}{4}} e^{-t/q\tau} \qquad t < q\tau$$

$$= q^{\frac{1}{4}} e^{(q-1)} e^{-t/\tau} \qquad t > q\tau$$

indicates that the prior time interval calculation is different depending on whether $S_o > q^{\frac{1}{4}}/e$ as shown in Figure 4 or $S_o < q^{\frac{1}{4}}/e$ as shown in Figure 5.

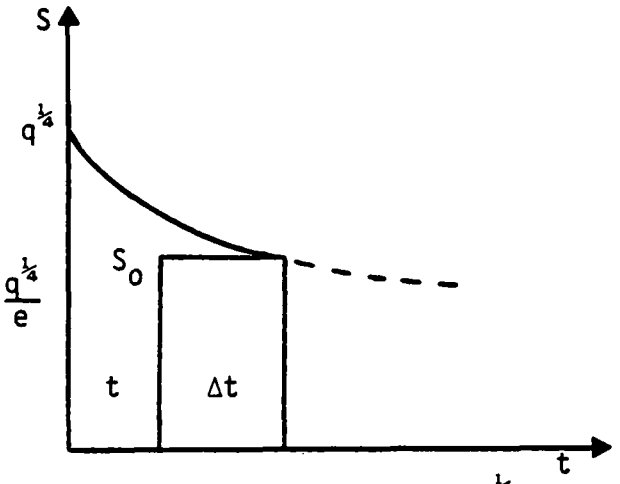

Figure 4. Overdense, $S_o > q^{\frac{1}{4}}/e$

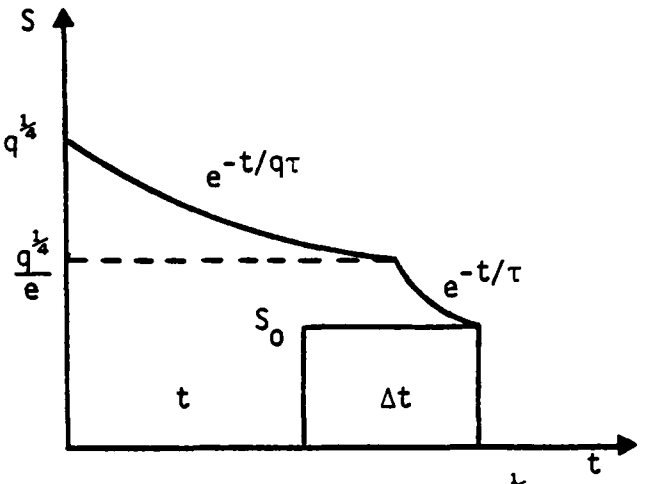

Figure 5. Overdense, $S_o < q^{\frac{1}{4}}/e$

For the general case of overdense trails, the integration will begin at $q_1 \geq 1$. We define $q_2 \equiv (eS_o)^4$. Then for $q_1 < q_2$ we have the situation of Figure 4 and

$$q_1 = S_o{}^4 e^{4\frac{\Delta t}{\tau q_1}} = q_2 e^{4\left[\frac{\Delta t}{\tau q_1} - 1\right]} .$$

This situation obtains if $\Delta t/\tau < q_2$. For $q > q_1$, the prior time interval in which the meteor is useful is given by

$$t = q\tau \, \ell n \left(\frac{q^{\frac{1}{4}}}{S_o}\right) - \Delta t \text{ until } q = q_2$$

or until $t(q)=T$ which occurs for

$$q_T^{\frac{1}{4}} e^{-\frac{(T+\Delta t)}{q_T \tau}} = S_o \quad .$$

For the case $q_T<q_2$ or $\left[\frac{T+\Delta t}{\tau}\right] <q_2$, we have

$$\overline{P_o}(S_o,\Delta t,T) = e^{-\left[\int_{q_1}^{q_T} \frac{M_o dq}{q^2}\left(q\tau \ \ell n\left(\frac{q^{\frac{1}{4}}}{S_o}\right)-\Delta t\right) + \int_{q_T}^{\infty} \frac{M_o dq}{q^2} T\right]}$$

$$= e^{-\frac{M_o\tau}{8}\left(\ell n^2(q_T)-\ell n^2(q_1)\right)} e^{M_o\tau \ \ell n(S_o)\ \ell n\left(\frac{q_T}{q_1}\right)} e^{\frac{M_o\Delta t}{q_1}} e^{-M_o(T+\Delta t)/q_T} \quad .$$

For $A = \frac{T+\Delta t}{q_T\tau}$ and $B = \frac{\Delta t}{q_1\tau}$

and the definitions of q_1 and q_T this can be put in the form

$$\overline{P_o} = e^{-M_o\tau(A-B)(1+2[A+B])} \quad .$$

For the case $\left[\frac{t+\Delta t}{\tau}\right] >q_2$

$q_T > q_2$ and we have the same integration until $q = q_2$. For $q>q_2$ we use

$$q^{\frac{1}{4}} e^{q-1} e^{-(t+\Delta t)/\tau} = S_o$$

or $t = \tau\left(q-1 + \ell n\left(\frac{q^{\frac{1}{4}}}{S_o}\right)\right) - \Delta t$ until q_M which occur for $q_M^{\frac{1}{4}} e^{q_M-1} e^{-(T+\Delta t)/\tau} = S_o$

so that

$$\overline{P_o} = e^{-M_o\tau\left[\frac{\ell n^2(q_2)-\ell n^2(q_1)}{8} - \ell n\,(S_o)\,\ell n\left(\frac{q_2}{q_1}\right)\frac{-\Delta t}{\tau}\left(\frac{1}{q_1}-\frac{1}{q_2}\right)\right]}$$

$$*e^{-M_o\tau}\int_{q_2}^{q_M}\frac{dq}{q^2}\left[q-1+\ell n\left(\frac{q^{\frac{1}{4}}}{S_o}\right)\frac{-\Delta t}{\tau}\right]e^{-M_oT/q_M}$$

The integral is $\ell n\left(\frac{q_m}{q_2}\right)+\left(\frac{1}{q_m}-\frac{1}{q_2}\right)\left(1+\ell n\,S_o+\frac{\Delta t}{\tau}\right)+\frac{1}{4}\left(\frac{\ell n(eq_2)}{q_2}-\frac{\ell n(eq_M)}{q_M}\right)$.

Since $q_M = q_2 e^{\frac{4(T+\Delta t)}{\tau}} - 4q_M$,

$$\frac{\ell n(eq_m)}{4q_m} = \frac{\ell n(eq_2)}{4q_m} + \left(\frac{T+\Delta t}{\tau q_m}\right) - 1$$

and by the definition of q_2 and q_1

$$\overline{P_o} = e^{-M_o\tau\left[3-B-2B^2+4q_m(c-1)+\frac{1}{4}\left(\frac{1}{q_2}-\frac{1}{q_m}\right)\right]}$$

where

$$C = \frac{T+\Delta t}{q_M\tau} \quad .$$

Finally for $\Delta t/\tau > q_2$, we have the situation of Figure 5 where

$$t(q) = \tau\left(q-1+\ell n\left(\frac{q^{\frac{1}{4}}}{S_o}\right)-\Delta t/\tau\right)$$

and the integration is between

$$q_3 = q_2 e^{4(\Delta t/\tau - q_3)} \text{ and } q_M$$

and $\overline{P_o} = e^{-M_o\tau\left[\ell n\left(\frac{q_m}{q_3}\right)+\left(\frac{1}{q_m}-\frac{1}{q_3}\right)\left(\ell n(eS_o)+\frac{\Delta t}{\tau}\right)+\frac{1}{4}\left(\frac{\ell n(eq_3)}{q_3}-\frac{\ell n(eq_M)}{q_m}\right)+\frac{T}{\tau q_M}\right]}$

which reduces to

$$\overline{P_o} = e^{-M_o\tau\left[\ell n\left(\frac{q_m}{q_3}\right)-\frac{1}{4}\left(\frac{1}{q_m}-\frac{1}{q_3}\right)\right]}$$

3. RESULTS

The implementation of the overdense formulas is described in Appendix B. We now illustrate the results of the new model for cases of interest previously described in Ref. 1.

Figure 6 is an illustration of a FFB-FFB link PMR vs. broadcast time for a value $P_t G_t G_r = 10^3$ watts. Two of the curves are the N=1 and N=8 packet cases of the old model. The third and lowest curve is the N=8 packet case treated by the new model. The N=1 case output is identical for the two models. We see the difference as negligible for this case since the meteor trails of importance are primarily underdense.

In that reference we suggested a scaling of power requirements with broadcast time as $P_t G_t G_r \, t^2$ = constant which comes from the theory of underdense trails. We therefore suggested that results for 1000 watts are identical to results for 250 watts if the time is doubled. We now show the underdense scaling to overstate performance when carried to powers as low as 250 watts. This results because the required trails are overdense at that power. Figure 7 shows the new results. The top two curves show the erroneously scaled results for one and eight packets. These are the same curves as in Figure 6 but the time scale (abscissa) has been doubled. For N=1, P=0.9 at t=8 min according to the old scaling.

The lower two curves are the actual results from the new model. The time for P=0.9 is much longer. For the N=1 case we can explain the difference. The probabilities depend on the product Mt where M, the useful burst rate, = M_0/q where q is the required strength. For 1000 watts, we had $q \approx 1/\sqrt{2}$ so $M = M_0\sqrt{2}$. The product P = 0.9 was $M_0 \sqrt{2}$ x 4 min. For 250 watts the required signal level was twice as high which would require $q = \sqrt{2}$ if underdense scaling were valid leading to a product $(M_0/\sqrt{2})t = M_0 \sqrt{2}$ x 4 or t=8 min for 250 watts. The new program recognized that overdense bursts are required for signal levels >1 so the required strength is $q^{\frac{1}{4}} = \sqrt{2}$ or q=4 leading to $M = M_0/4$. The required product $(M_0/4)t = M_0\sqrt{2}$ x 4 or $t = 16\sqrt{2} = 22.6$ min as seen in Figure 7. This scaling argument may hold for N=1 since the time-dependent form of the trail signal is not important if $\Delta t \ll \tau$ which is the case here. For N=8, $8\Delta t \approx \tau$ and the different time dependences of over- and underdense trails complicate the problem and the

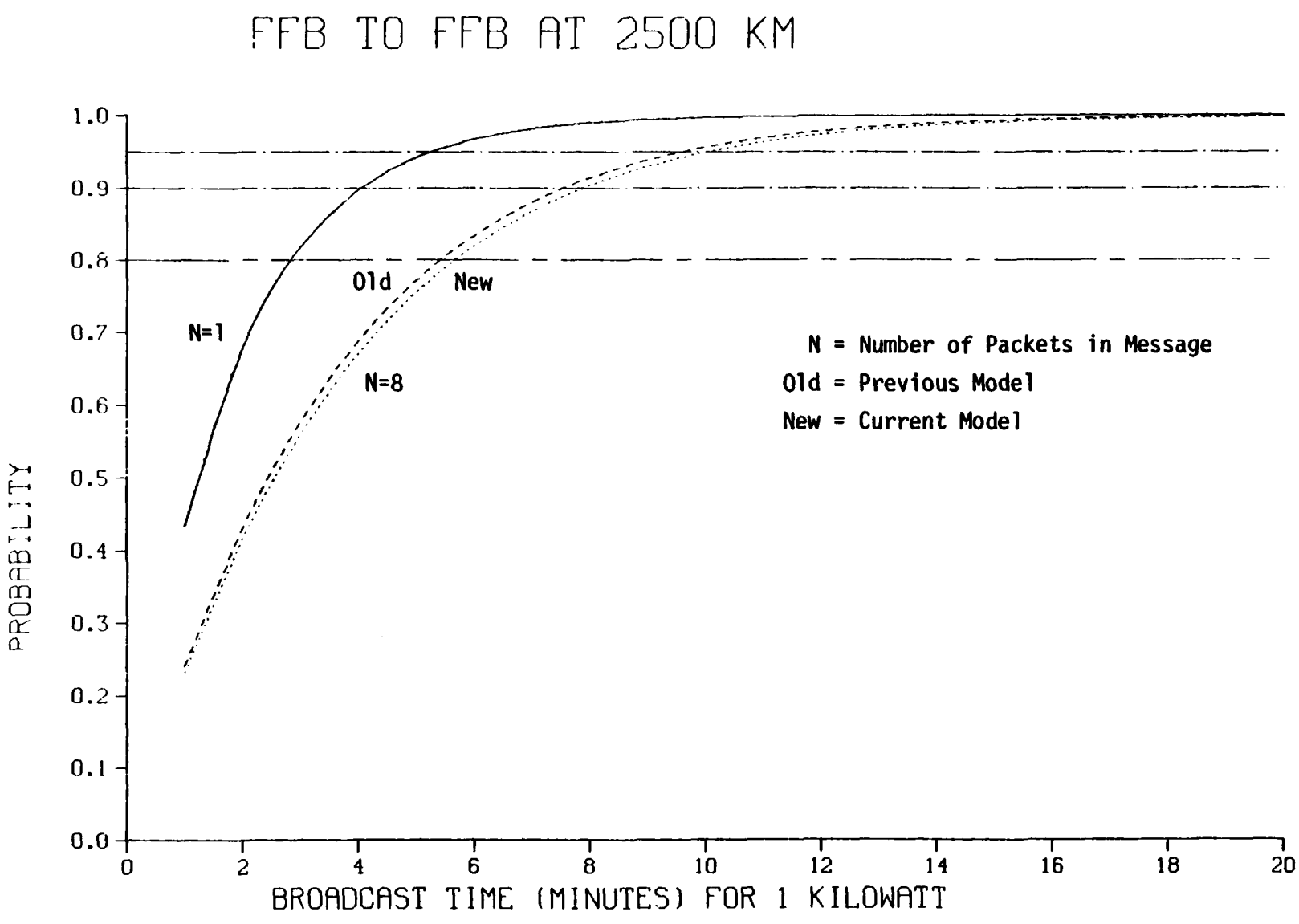

Figure 6. Probability of Correct Message Receipt Vs. Broadcast Time FFB-FFB; $P_t G_t G_r$ = 1000 W.

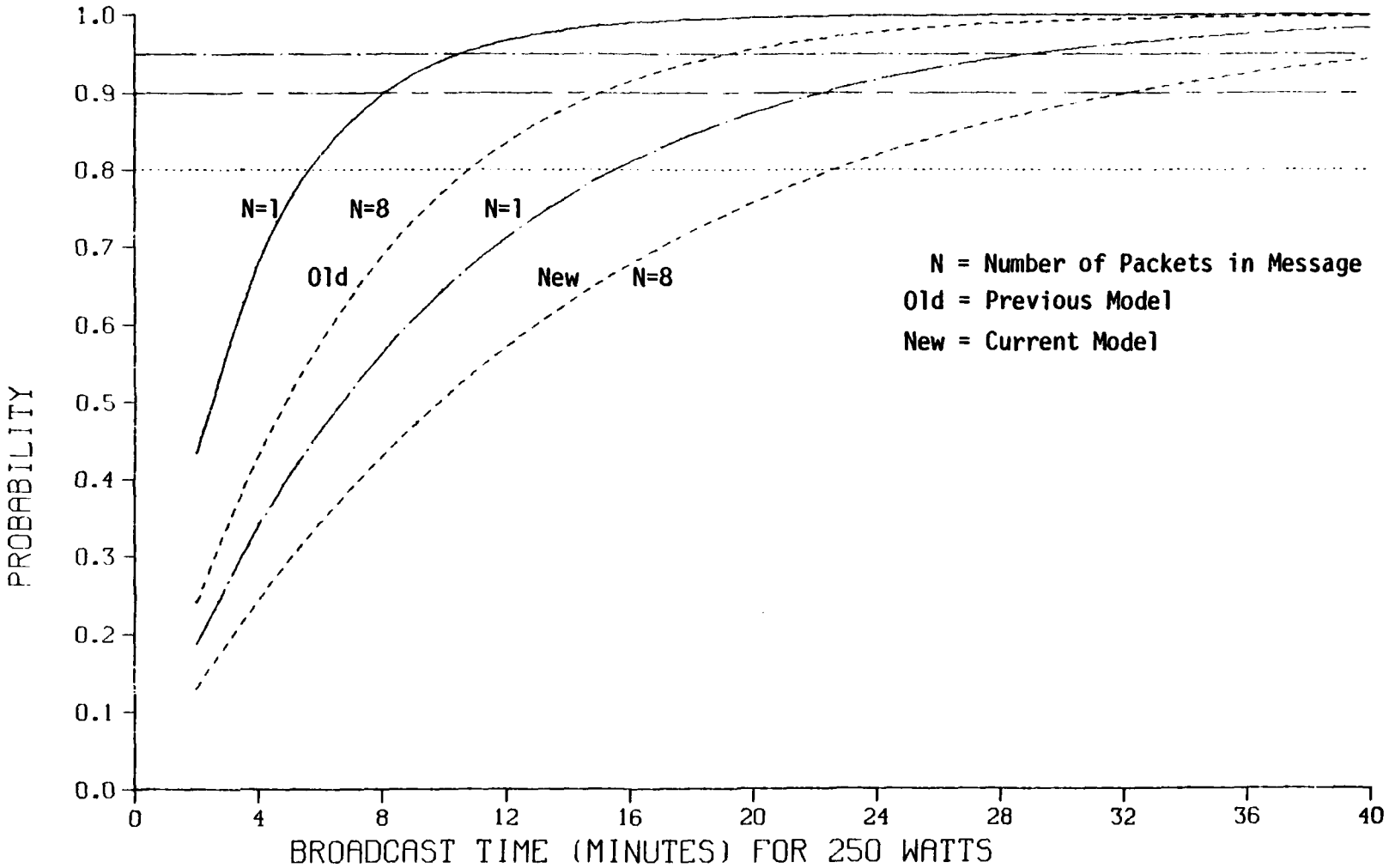

Figure 7. Probability of Correct Message Receipt Vs. Broadcast Time FFB-FFB, $P_t G_t G_r$ = 250 W.

scaling argument becomes inaccurate. This new scaling argument is also inaccurate for any N for the break point case of 500 w. For this case the underdense scaling argument would say the required strength is q=1 leading to $t = 4\sqrt{2} = 5.66$ min. The N=1 and 8 cases are shown in Figure 8 for 500 watts. The actual time to achieve P = 0.9 with N=1 is approximately 7 min when overdense trails are considered.

The reason for this discrepancy is that $\Delta t/\tau$ is finite. For finite $\Delta t/\tau$, the minimum strength required is

$$q = S_o e^{\Delta t/\tau} \quad q < 1$$

$$q = S_o{}^4 e^{\frac{4\Delta t}{q\tau}} \quad q > 1$$

For $\Delta t/\tau = 0.1$ we have

$$q(1000) = \frac{1}{\sqrt{2}} e^{0.1} \approx \frac{1}{\sqrt{2}}$$

$$q(250) = (\sqrt{2})^4 e^{\frac{4\Delta t}{q\tau}} \approx 4\, e^{\frac{4\Delta t}{4\tau}} \approx 4\, e^{0.1} \approx 4$$

so the scaling that ignores $\Delta t/\tau$ is adequate. But $q(500) = e^{\frac{4\Delta t}{q\tau}} = e^{\frac{0.4}{q}}$ is not accurately approximated by q=1. The answer is q = 1.346.

We therefore abandon scaling arguments and use output curves of probability of message receipt vs. power for a five minute and ten minute broadcast time. Figures 9-14 show the results for the two times and the three cases of FFB-FFB at 2500 km, FFB-GRD, and GRD-GRD at 1400 km. These three cases were represented in the power requirements section of Ref. 1. We replace the values of radiated power given in Table 5-2 of that reference with the values obtained from the N=7 curve in Figures 9-14. In these figures, the abscissa is the power factor $P_t G_t G_r$ for the FFB-FFB and GRD-GRD cases but is $P_t G_t$ for the FFB-GRD case where an average over range was done. For that case, G_r vs. angle was included in the averaging. We show the new values in Table 1 where we assume 5 dB gain for surface antennas and 0 dB gain for the FFB antenna.

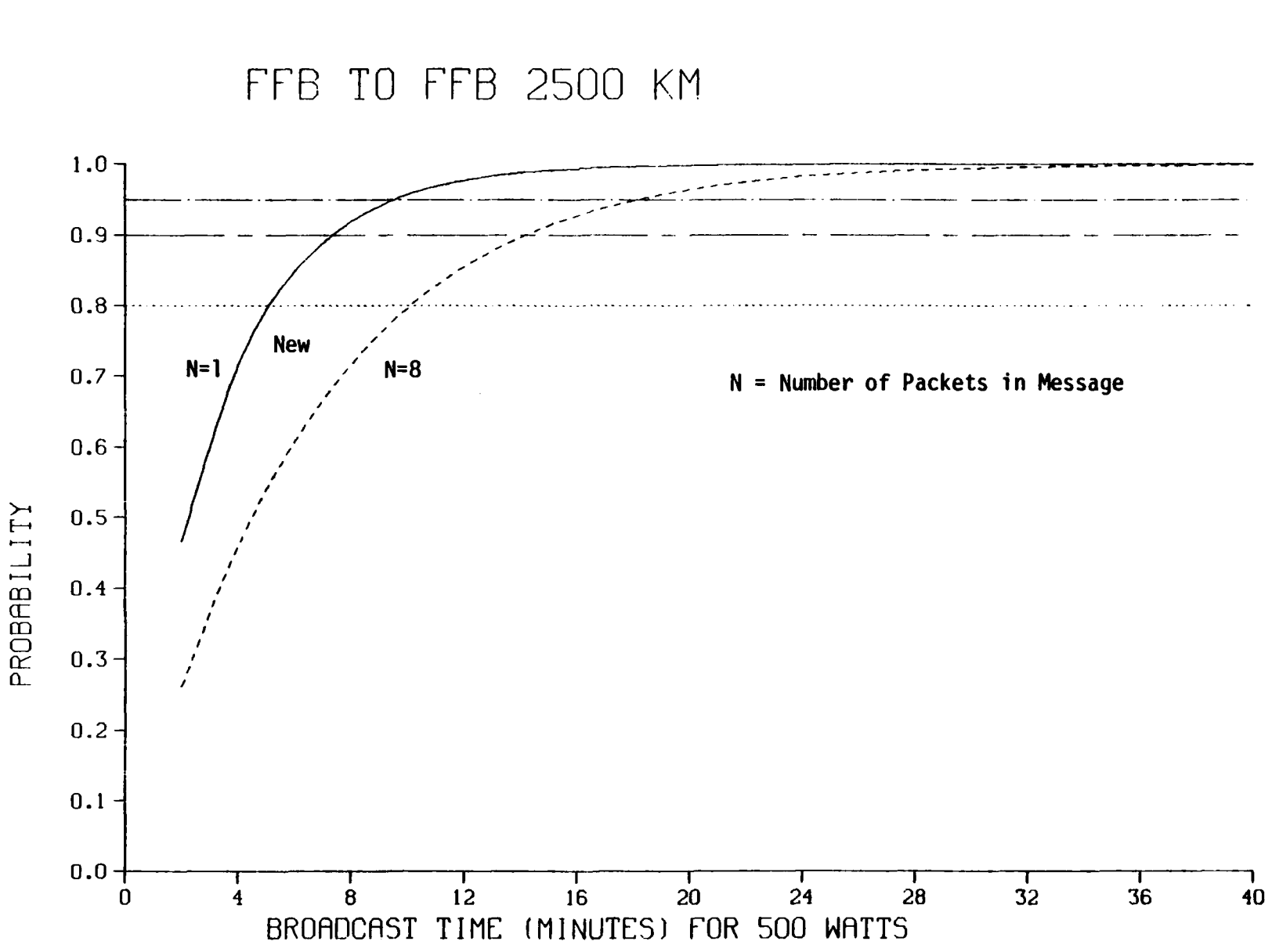

Figure 8. Probability of Correct Message Receipt Vs. Broadcast Time FFB-FFB; $P_t G_t G_r$ = 500 W.

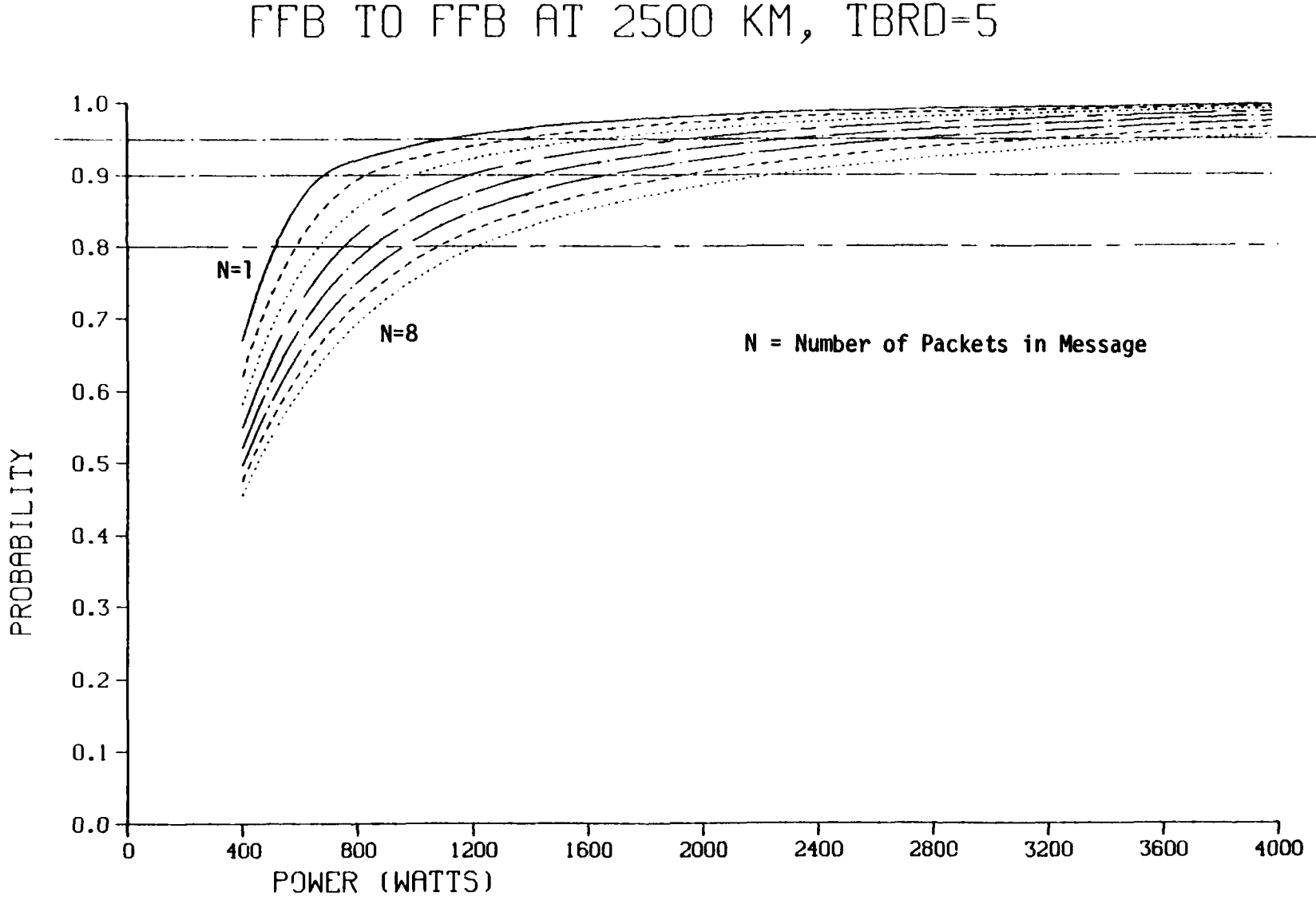

Figure 9. Probability of Correct Message Receipt Vs. Power Factor $P_t G_t G_r$; FFB-FFB; Broadcast Time = 5 min.

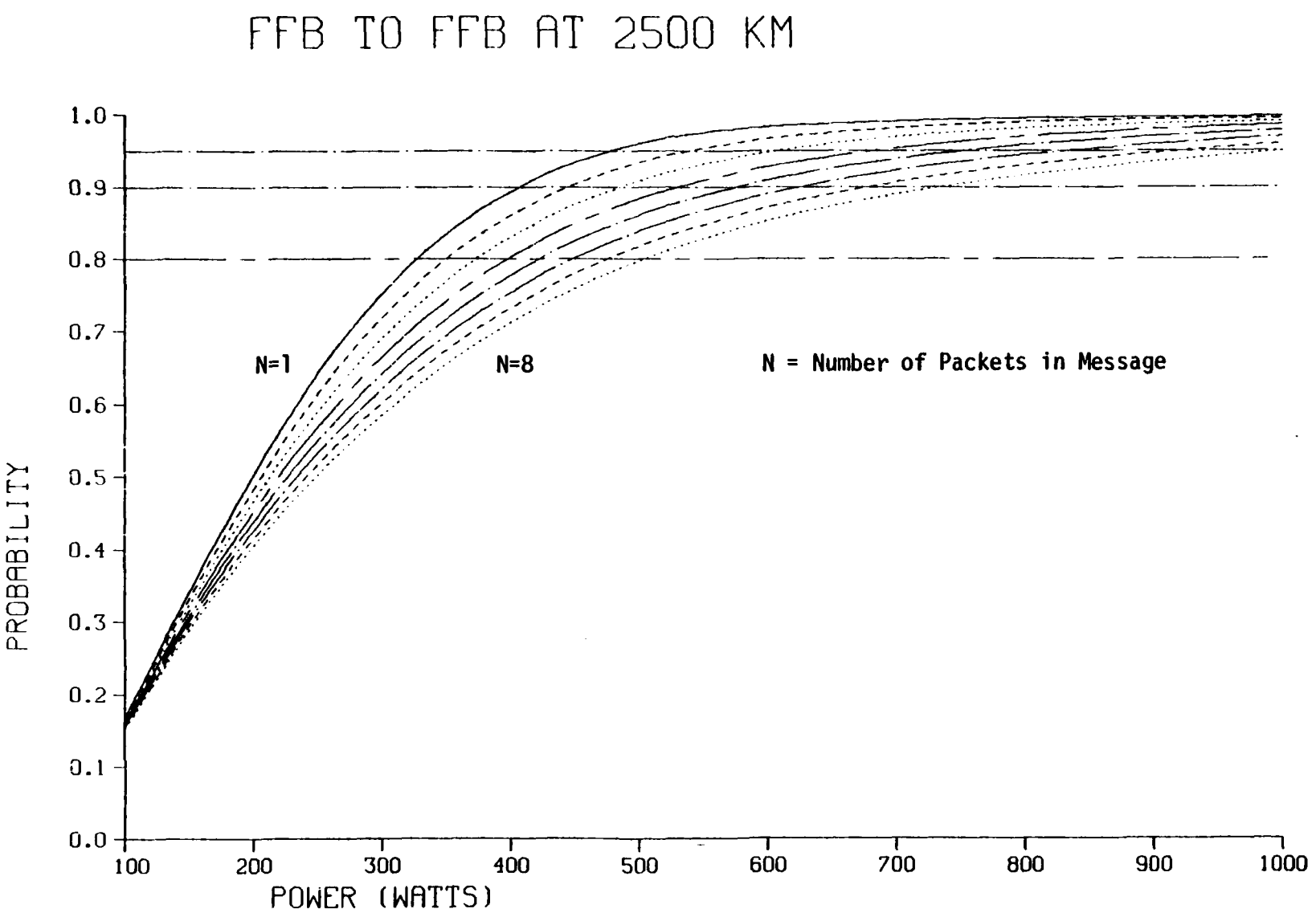

Figure 10. Probability of Correct Message Receipt Vs. Power Factor $P_t G_t G_r$; FFB-FFB, Broadcast Time = 10 min.

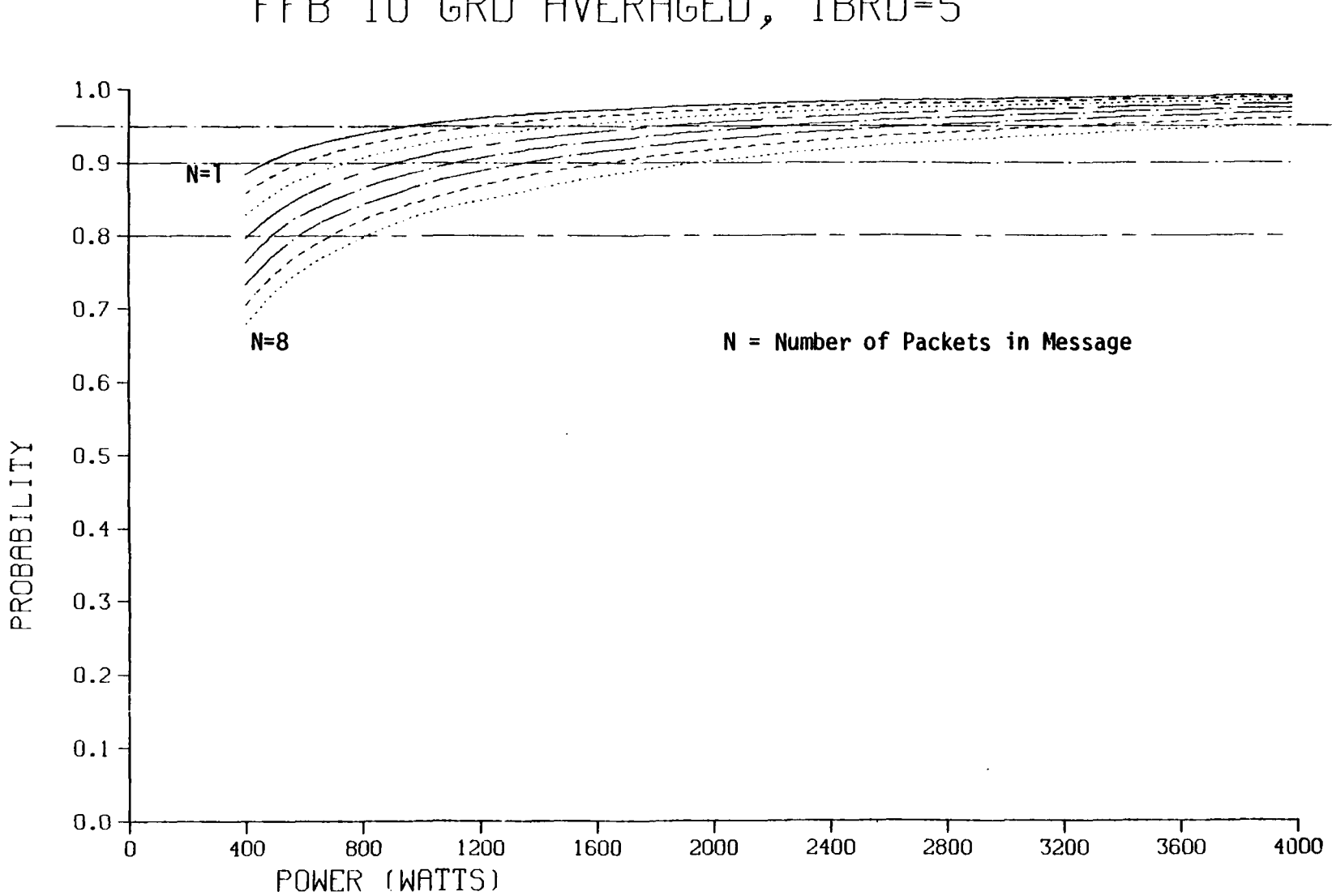

Figure 11. Probability of Correct Message Receipt Vs. Power Factor $P_t G_t$; FFB-GRD; = 5 min.

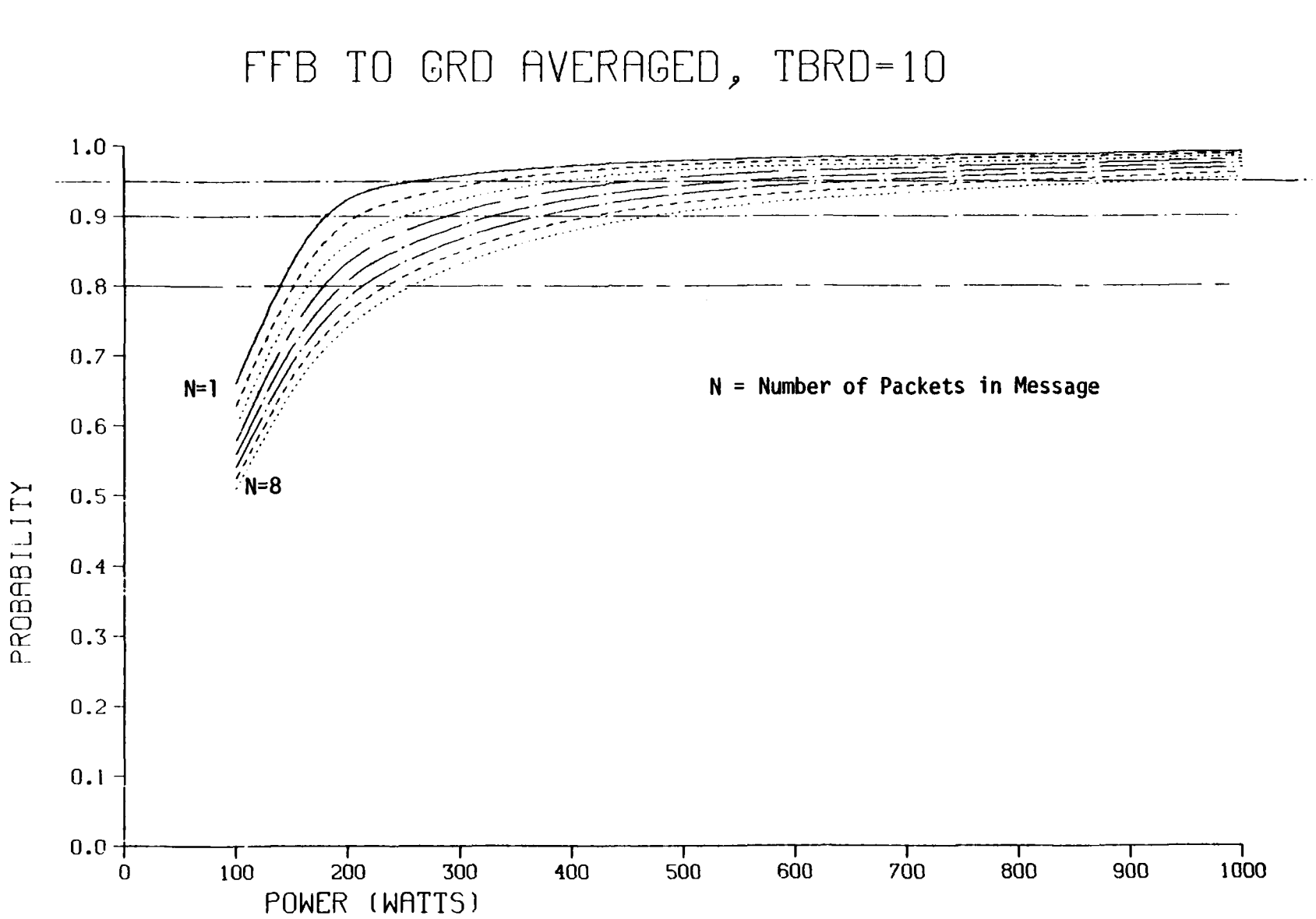

Figure 12. Probability of Correct Message Receipt Vs. Power Factor P_tG_t; FFB-GRD; Broadcast Time = 10 min.

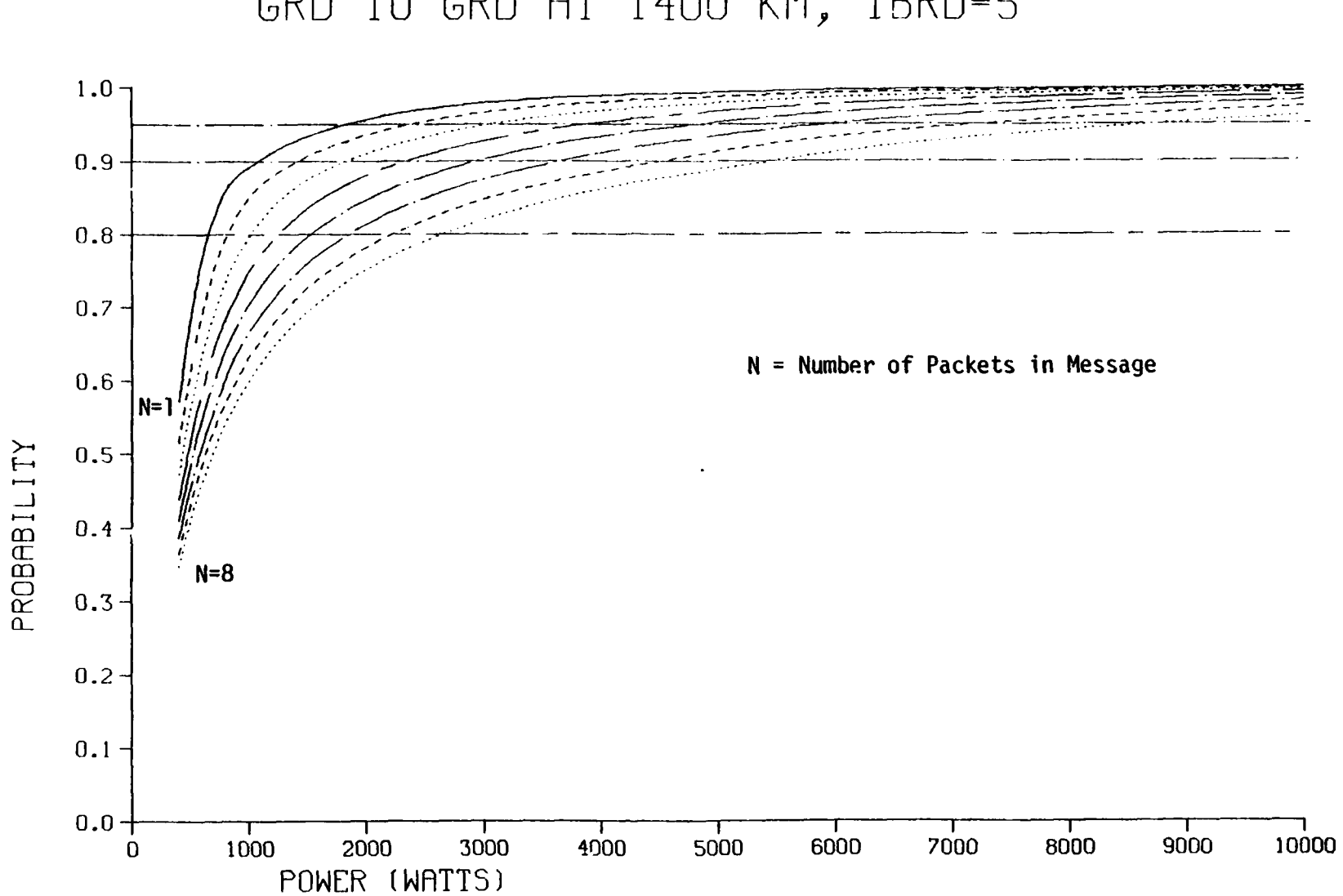

Figure 13. Probability of Correct Message Receipt Vs. Power Factor $P_t G_t G_r$; GRD-GRD; Broadcast Time = 5 min.

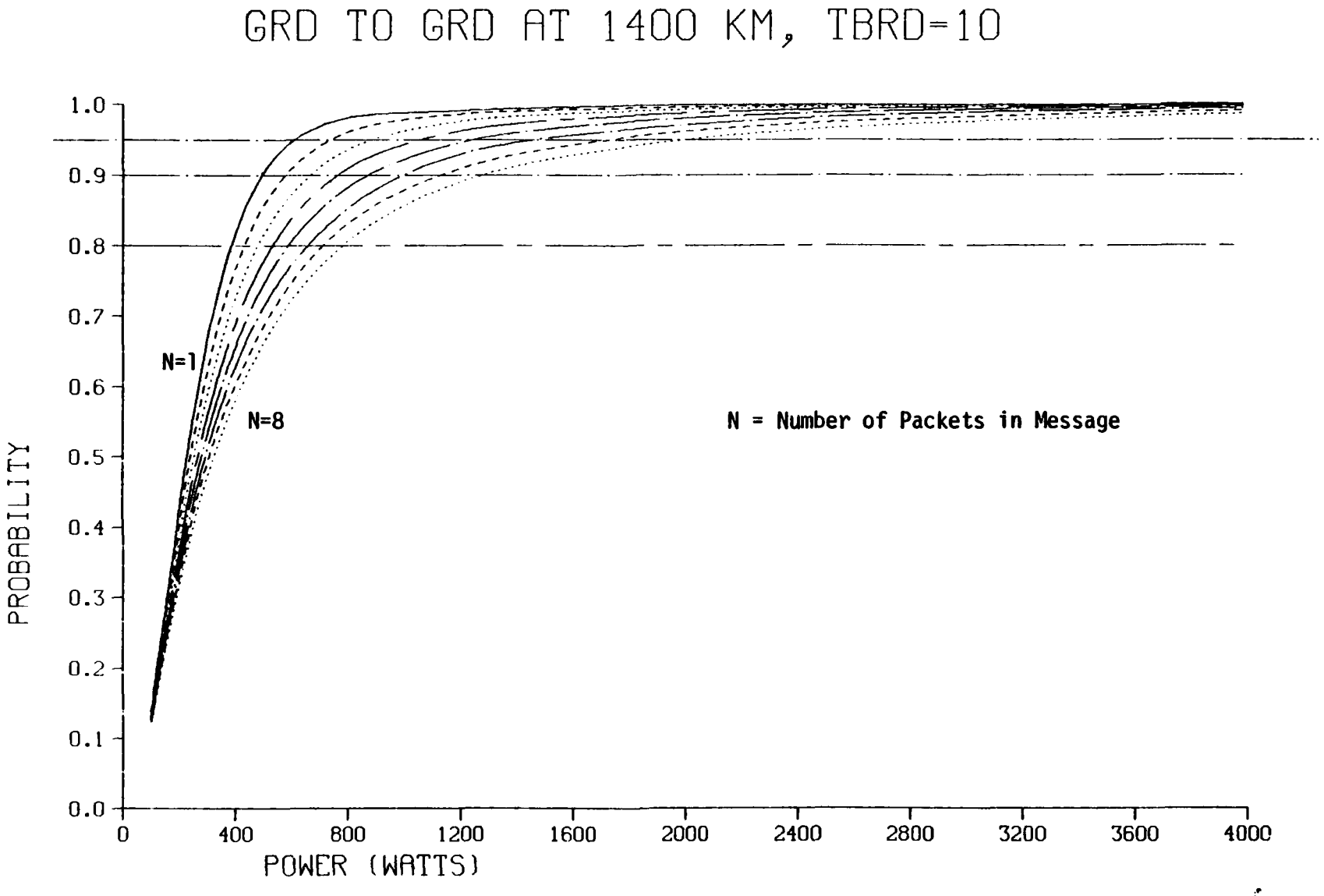

Figure 14. Probability of Correct Message Receipt Vs. Power Factor $P_t G_t G_r$; GRD-GRD; Broadcast Time = 10 min.

Table 1. Radiated Power as a Function of Link Connectivity and Broadcast Time Using Improved Model

Type	Radiated Power (watts)			
	PMR =	80%	90%	95%
FFB-FFB	5 min	1100	1950	3200
	10 min	475	675	910
FFB-Surface	5 min	700	1640	3200
	10 min	240	420	800
Surface-Surface	5 min	220	450	725
	10 min	70	110	172

For the case of the buoy, we are interested in lower powers and longer broadcast times. We therefore include in Figures 15 and 16 the cases of 1400 km GRD-GRD for 30 and 60 minutes respectively. Using 5 dB gain for the receiving radiated power for various probabilities of message receipt for various broadcast times in Table 2.

We find power requirements in Tables 1 and 2 to be higher than that previously posed only at the lower values of power as in the 10 min FFB-FFB case and in the 30 and 60 min cases for the buoy. As previously mentioned, at values of $P_t G_t G_r \geq 1000$ w the old model based upon underdense theory is adequate. It may even be conservative since at large values of T and lower values of S_o, the fact that overdense bursts have longer time constants can overcome their relative rarity by their higher useful life. In fact, the prior time T used in this analysis should be limited to a few seconds because trails more than several seconds old are unreliable because of the multipath effects due to wind-shear distortion of the trail. This did not impact our analysis since the largest trail time we use is $T+\Delta t = 9\Delta t = 1.097$ s.

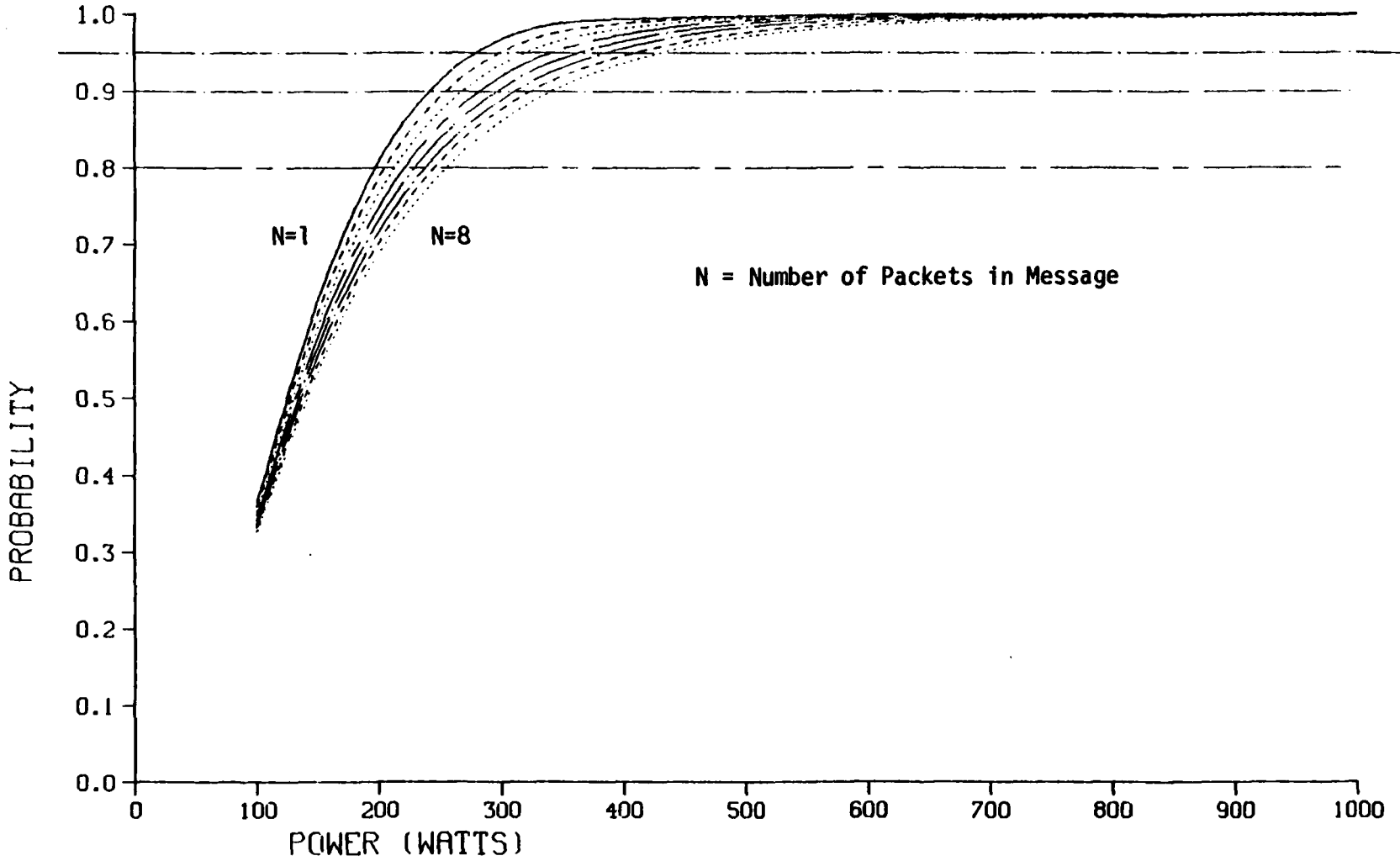

Figure 15. Probability of Correct Message Receipt Vs. Power Factor $P_t G_t G_r$; GRD-GRD; Broadcast Time = 30 min.

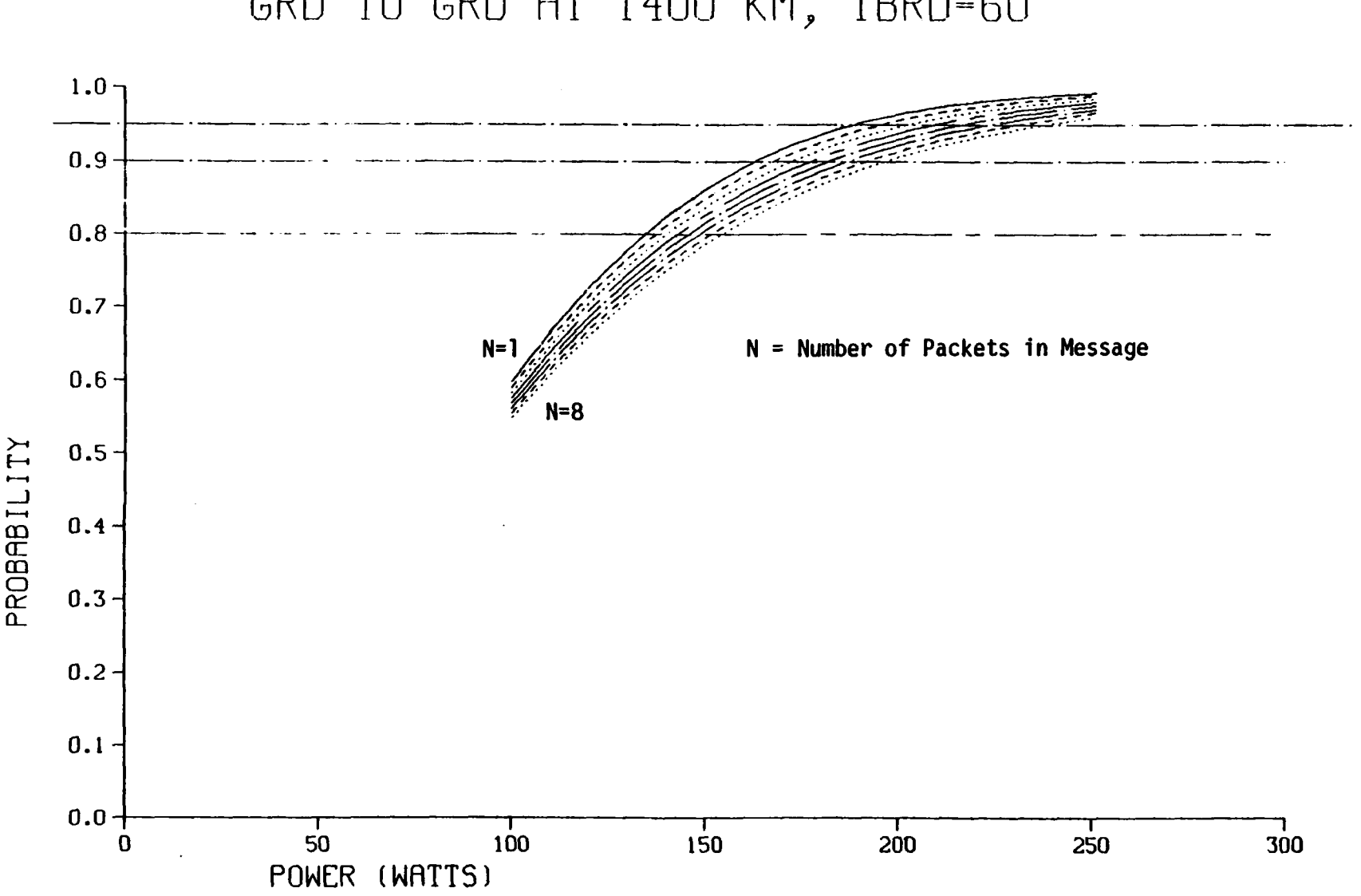

Figure 16. Probability of Correct Message Receipt Vs. Power Factor $P_t G_t G_r$; GRD-GRD; Broadcast Time = 60 min.

Table 2. Radiated Power as a Function of Link Connectivity and Broadcast Time for Buoy-Surface Using Improved Model

Radiated Power (watts)			
PMR =	80%	90%	95%
5 min	464	949	1530
10 min	148	232	363
30 min	52	67	84
60 min	32	40	47

REFERENCES

1. "Stratsec Functional/Performance Allocation Analysis (U)," SAI, La Jolla, CA, SAI LJ DC #83:0835 prepared under Contract N00039-81-C-0654 for NAVELEX, PME 110 (July 1983). (C)

2. Sugar, George, R., "Radio Propagation by Reflection from Meteor Trails," Proc IEEE, vol. 52, 2, p. 116-137, February 1964.

3. Final Report, "Analysis of Meteor Burst Communications for Navy Strategic Applications," for Naval Ocean Systems Center, Contract No. N66001-79-C-0460, February 4, 1980.

4. Shoemaker, R. M., H. E. R. Jones, "Tactical Application of Burst Type Meteor-Trail Communications", Litton Data Command Systems, Agoura, California.

APPENDIX A
VHF(MB) Link Performance Model

The VHF(MB) model is based on test system data described in Refs. 1 and 2 for surface-to-surface links. The effects of elevating one or both antennas is estimated from geometrical considerations. These aspects of the model are easily modified as more data become available.

The model output is the probability of message receipt (PMR) within a continuous broadcast time t. The message may be in a single packet of time-length Δt sec. The message is not considered received unless the meteor burst trail is of sufficient cross section and duration to reflect the entire message. For a message consisting of N packets, the probability of message receipt is defined as the probability of receiving all N packets in any order within the broadcast time.

The model is based on the physics of underdense reflection of radio signals as described in Ref. 3. An underdense trail's diffusive time spread causes the received signal strength to decay exponentially with characteristic time

$$\tau = \frac{\lambda^2 \sec^2 \phi}{16 \pi^2 D} \quad \text{(sec)}$$

where λ = wave length (m)

D = diffusion coefficient (m^2/sec).

In the model, $D = 8$ m^2/sec as used in Ref. 1 and ϕ, the half angle of scatter at the trail, is calculated for a meteor burst at 100 km altitude midway between antennas. Antenna heights are zero for surface and 21.3 km for balloon. For surface-balloon links, the calculation uses half the height of balloon.

Although useable meteor trails occur over a large portion of the sky, the most likely occurrences are near the midpoint[3] so this point is used for scaling purposes.

When $\Delta t << \tau$, a meteor trail with electron line density, q, high enough to scatter the required signal strength at the receiver, will reflect the entire message. We designate the average rate of occurrence of one or more bursts with this value q or higher as M_o (bursts/min).

It is known[3] that this burst rate is proportional to 1/q. For under-dense bursts, the scattered signal strength is proportional to q. Reference 1 outlined a method of scaling from their test system to any other test system operating at optimum ground ranges. For a required receiver threshold T_r (watts) which sets the required signal strength T_r, and given values of transmitter gain, G_t, above an isotrope, transmitter radiated power, P_t, and receiver gain, G_r, above an isotrope, the required value of q is proportional to

$$\sqrt{\frac{T_r}{P_t G_t G_r \lambda^3}}$$

from the transmission equation.[1,2,3] This equation is shown later in the text. The gains correspond to directions from antenna to meteor burst which are taken at the midpoint of the range. Therefore the rate of useful meteors,

$$M_o \propto \sqrt{\frac{P_t G_t G_r \lambda^3}{T_r}} .$$

For the test system,[1]

$$\lambda = 6.383\text{m}$$

and

$$\frac{P_t G_t G_r}{T_r} = 10^{18}$$

The values of M_o for the test system ranged from a daily minimum of 19/hour to 25/hour depending on season. The daily median value ranged from 50 to 70/hour. We have chosen a conservative value of 40/hour = 2/3 / minute for the model.

It is known[1,2,4] that surface-to-surface meteor burst performance is best at midranges but degrades at larger ranges because of earth curvature and at shorter ranges because of geometric and depolarization effects. The useful meteor rate calculated is therefore modified according to range and link geometry.

A linear fall off of useable meteors with range is used to model the decrease in the volume of useable meteor trails as the bulge of the earth shadows the line of sight. If one degree elevation is used as the limit below which signal strength drops quickly, the groundrange at which a meteor trail altitude of 100 km reaches this elevation is 1000 km for an antenna on the earth's surface. We therefore choose 2000 km range between surface antennas as a cut off. The actual horizon (0° elevation) is at 1130 km. According to Oetting,[4] a fit to data from Boeing Alaska tests[2] shows the meteor rate at large ranges to be constant for 770<R<1280 km and to fall off for R>1280 km. We therefore linearly degrade the meteor rate to zero at 2000 km from its value at 1280 km. For R<770 km, we use Oetting's scaling from the tests from 770 km down to the range of 200 km where the ground wave is of sufficient strength to preclude the need of a meteor burst. This scaling from data shows the meteor rate reduced a factor 480/770 for R<480 km and rising as R/770 to the constant value for 480<R<770 km.

For the case of a surface to balloon link, the ground wave can be of sufficient strength for a much larger range. The line-of-sight from a balloon at 21.3 km altitude grazes the earth at a range of 520 km. Without the appropriate formulas for signal strength vs. range for the various geometries, we assume that 200 km of further ground range can be added to this so that meteor bursts are not needed out to a range of 720 km. Beyond this range, the effec-

tive meteor burst rate will be taken as constant as in the surface-surface case until the earth's bulge effect sets in wherein a linear fall to zero at some maximum range is effected. The line-of-sight from a balloon to a meteor trail grazes the earth at a combined range of 520+1130 = 1650 km from balloon to trail. Since we choose 1000 km as the maximum range from a surface antenna to the meteor trail, the total cut off range for surface to balloon is 1650+1000 = 2650 km.

The determination of the range where the fall off in useful meteor trails begins requires a knowledge of the distribution of the trails over the sky at 100 km altitude. The only case where this distribution is given in the literature is for surface-to-surface at 1000 km range. This shows the bulk of the useful trails to be near the midpoint of the sky between the antennas. This should be also true at greater ranges. Therefore the fall-off with range should be small until the final area becomes shadowed. If this area is similar in range extent to that of the surface-surface case, the range over which the fall-off occurs should be similar. We therefore begin the linear fall-off 720 km in from the maximum range of 2650 km at 1930 km. Similarity in range extent is consistent with using the same constant meteor rate for both surface-surface and surface-balloon geometries.

For the balloon-balloon case we consider ground wave operable to a range of 520+520+200=1240 km. The cut off for meteor bursts will be at the maximum range 1650+1650=3300 km. We take the meteor burst rate as the same constant out to a range 3300-720=2580 km where the linear decline begins. Figure A-1 illustrates the modeled range dependence of M_o for the three cases.

For ranges less than shown in the figure where meteor bursts are not needed, the model returns a probability of message receipt of unity. For ranges greater than shown in the figure, the model returns a probability of zero. The geometries for the minimum and maximum ranges are shown in Figure A-2.

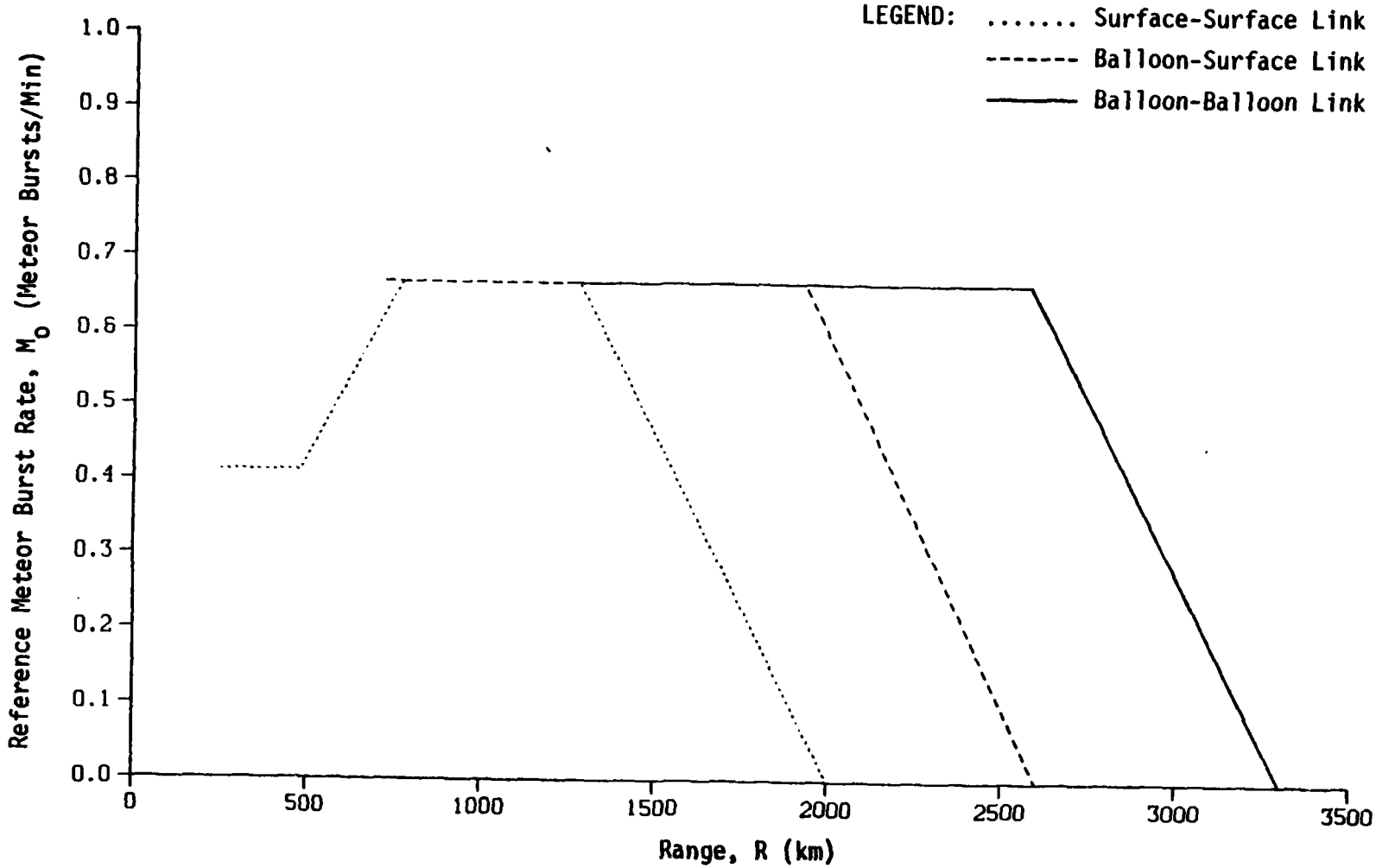

Figure A-1. Reference Useful Meteor Burst Rate.

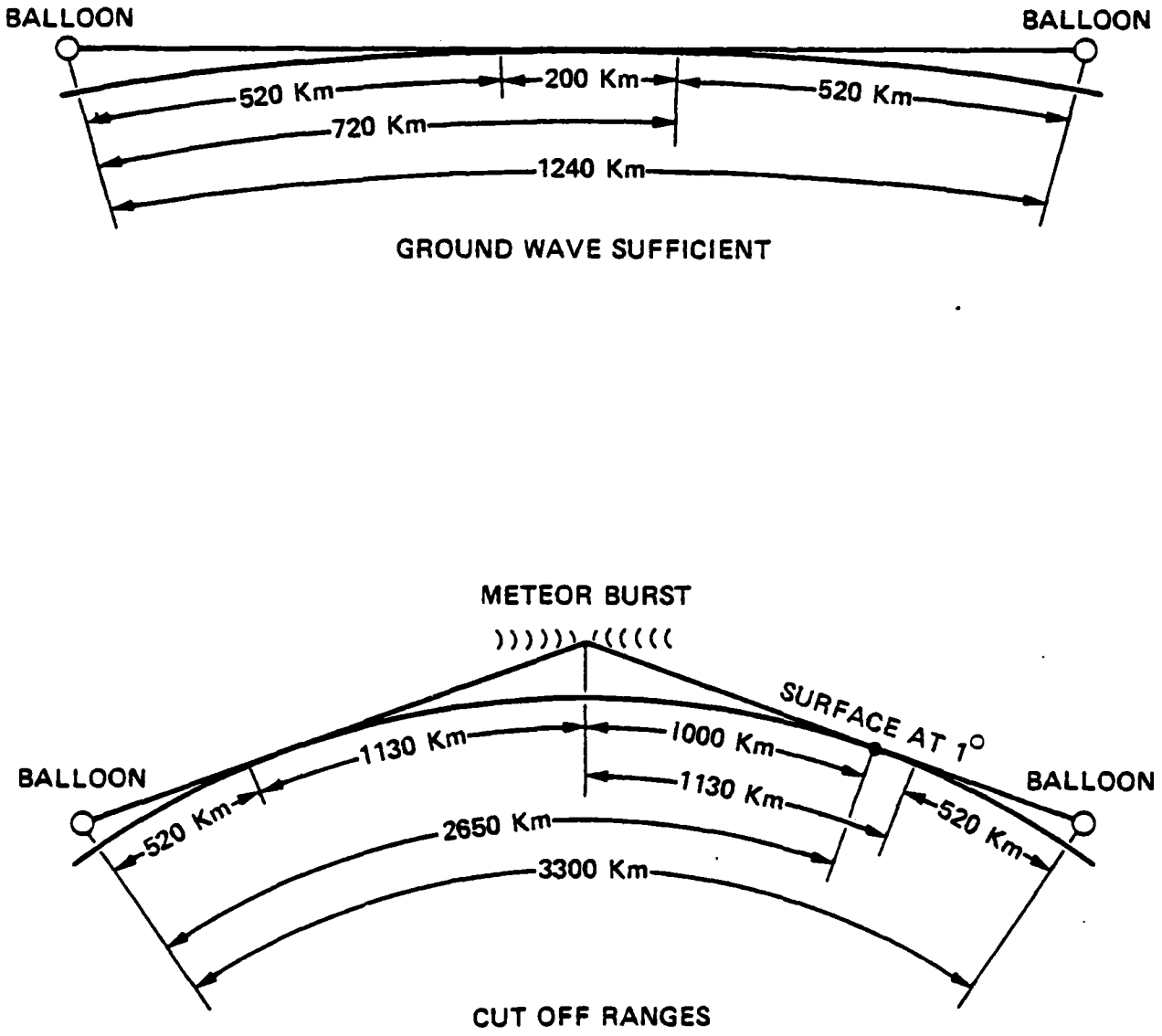

Figure A-2. Range Limits for Meteor Burst Communications.

The useable meteor rate for the system of interest is obtained by scaling

$$M = M_o \sqrt{\frac{P_t G_t G_r}{T_r \cdot 10^{18}} \left(\frac{\lambda}{6.383}\right)^3}$$

In using the model in this paper, the systems considered had $\lambda = 6.383$m and a receiver detection threshold[1] of $T_r = 10^{-15} \left(\frac{\text{data rate}}{4000 \text{ bits/sec}}\right) \left(\frac{\lambda}{6.383}\right)^{2.3}$ watts for a bit error rate of 10^{-3} for coherent PSK.

The useable meteor rate therefore scales as $M = M_o \sqrt{P_t(kW)\ G_t\ G_r}$ for $\lambda = 6.383$ m and data rate = 4000 bits/sec.

The scaling of M and the exponential time dependence of the signal which will be used in deriving the PMR output of this model is valid only for underdense meteor burst trails. If underdense, the signal level has a value and time dependence which varies as

$$r_e q e^{-t/\tau}$$

where $r_e = 2.8 \cdot 10^{-15}$m = classical electron radius.

If overdense the variation[3] is

$$\frac{1}{\sqrt{4\pi}} \left[\frac{t}{\tau} \ln\left(\frac{4 r_e q \tau}{t}\right)\right]^{1/4}$$

which rises to a maximum at $t = \frac{4 r_e q \tau}{e}$ of value $\left(\frac{r_e q}{4\pi^2 e}\right)^{1/4}$

and drops to zero at $t = 4\, r_e q\tau$ at which time the trail is completely underdense. If $4r_e q<1$ or $q<10^{14}/m$, the underdense description should be adequate and conservative. If the power factor, $P_t G_t G_r$, is so low that a large $q>10^{14}/m$ is required, the model will have to be extended to include overdense reflections. Further analysis is required to determine the limit of applicability accurately in terms of system parameters. An estimate can be made from the transmission equation[1,2,3]

$$\frac{P_t G_t G_r}{16\pi^2}\ \lambda^3 q^2 r_e^{\,2}\ \left[\frac{\sin^2\alpha}{R_t R_r (R_t+R_r)(1-\cos^2\beta\ \sin^2\phi)}\right] = T_r$$

where α, the angle between the electric vector at the meteor trail and R_r, the direction vector from meteor trail to receiver, is a measure of depolarization loss. The distance from transmitter to meteor trail is R_t and β is the angle between the trail and the plane of R_t and R_r. The factor in brackets diminishes only slightly with range since α and ϕ get larger with range. If $\beta=0$, the bracket is $\sim 10^{-8}$ km^{-3} at the limit of large range $\sim$2000 km for which

$$P_t G_t G_r = \frac{60 \text{ watts}}{q^2 r_e^{\,2}}$$

for λ = 6.383m and $T_r = 10^{-15}$ watts. The transition point $qr_e = 1/4$ occurs for $P_t G_t G_r$ = 1 kilowatt at 2000 km where the earth bulge has no usable meteors anyway. At 1200 km range, the bracket is $\sim 2\cdot 10^{-8}$ km^{-3} and the transition point occurs for $P_t G_t G_r$ = 500 watts. Until more analysis and data comparison is done we should consider $P_t G_t G_r$ = 500 watts as a lower limit for validity of the model for long ranges. At shorter ranges, the model is valid at lower power factors.

We now derive the formulas for the PMR from the meteor burst parameters M and τ and the system parameters Δt, N and t. In the derivation we will redefine M as M_0 so as to define a new $M = M_0 e^{-\Delta t/\tau}$.

Consider a message of time length Δt. For any set of parameters describing the communication system there is a required minimum electron line density of the meteor trail for the successful receipt of a short message ($\Delta t \to 0$). The reflecting ability of the trails decreases exponentially with time with a time constant τ. If a message is not considered received unless its entire length is received continuously, the minimum strength of the meteor trail must be increased a factor $e^{\Delta t/\tau}$ for a meteor burst occurring just before the message. If the message is continuously repeated for a time t and the message is considered received if any length Δt or better within the message train is received during the transmission, the probability of receipt is calculated as follows.

The average rate of occurrence of meteor bursts with a specified strength or better is inversely proportional to strength. Therefore if M_o is the rate of required meteor bursts for $\Delta t=0$, $M=M_o e^{-\Delta t/\tau}$ is the rate for $\Delta t \neq 0$.

The probability that a useful meteor will occur in the short time dt is Mdt. The probability that one or more useful meteors will occur in a longer time t is $1-\bar{P}(t)$ where $\bar{P}(t)$ is the probability that no useful meteor occurred. $\bar{P}(t)$ is calculated as the product of the probabilities of N independent events. Each event is the nonoccurrence of a useful meteor in the time interval t/N with event probability (1 - Mt/N).

$$\text{Then} \qquad \bar{P}(t) = \lim_{N \to \infty} \prod_{i=1}^{N} \left(1 - \frac{Mt}{N}\right) = e^{-Mt}$$

Suppose instead that the message is sent only once. Reception requires a meteor burst of required strength or better just before the message or one stronger by $e^{dt/\tau}$ a time dt earlier and as prior time goes on the required strength increases exponentially. Suppose prior to some time t before the message began there were no meteors of the required strength. We can then break the interval as before but in this case

$$\bar{P}(t) = \lim_{N\to\infty} \prod_{i=1}^{N} \left(1 - \frac{Mt}{N} e^{-it/N\tau}\right)$$

Here the probability of nonoccurrence approaches unity as the position of the time interval recedes many time constants prior to the message.

$$\ln \bar{P} = \lim_{N\to\infty} \sum_{i=1}^{N} \ln \left(1 - \frac{Mt}{N} x^i\right); \quad x = e^{-t/N\tau}$$

$$\ln \left(1 - \frac{Mt}{N} x^i\right) = \frac{-Mt}{N} x^i + O\left(\frac{1}{N^2}\right)$$

$$\sum_{i=1}^{N} x^i = \frac{x - x^{N+1}}{1-x}$$

$$\ln \bar{P} = \lim_{N\to\infty} \frac{-Mt}{N} \frac{e^{-t/N\tau}\,(1-e^{-t/\tau})}{1-e^{-t/N\tau}}$$

$$= -M\tau\,(1-e^{-t/\tau}).$$

$$\bar{P}(t) = e^{-M\tau(1-e^{-t/\tau})}$$

which becomes independent of t for large t/τ. Therefore the probability of receiving the message is $P = 1-\bar{P}(\infty) = 1 - e^{-M\tau}$.

If the message is sent J times in a string with repetition period $T = N\Delta t$ the probability of not receiving the first and second transmissions of the message is the probability of not receiving the first times the probability of not receiving the second if the first wasn't received. If the first wasn't received, no burst of adequate or higher strength occurred. Therefore, certainly no burst of strength adequate or higher for the second occurred.

Therefore, no meteors occurred of the required strength prior to T before the second transmission. The probability of not receiving either is then

$$\bar{P}(1,2) = \bar{P}(\infty)\ \bar{P}(T) = e^{-M\tau(2-e^{-T/\tau})}$$

If we figure the total transmission time in complete periods, $t = JT = JN\Delta t$, the probability of not receiving any of the J transmissions is

$$\bar{P}(J) = \bar{P}(\infty)\ \bar{P}(T)^{(J-1)} = e^{-M\tau e^{-T/\tau}}\ e^{-M\tau J\ (1-e^{-T/\tau})}\ .$$

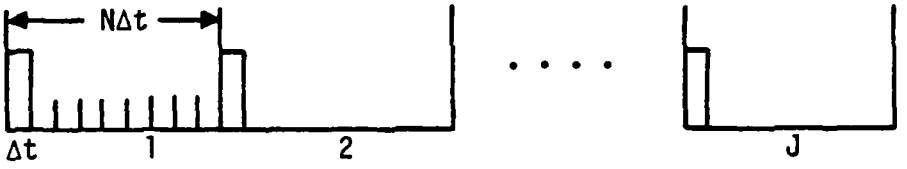

If two messages separated by $(p-1)\Delta t$ spaces are continuously sent in a packet of length $N\Delta t$ ($1 \leq p \leq N-1$), the probability of not receiving both messages if J packets are sent is

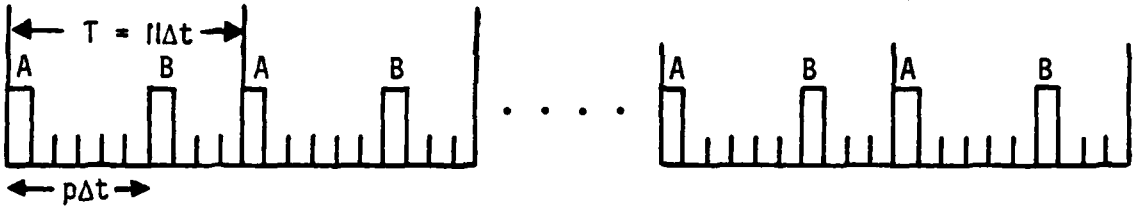

$\bar{P}(\bar{A}$ or $\bar{B}) = \bar{P}(J) + \bar{P}(J) - P(\bar{A}$ and $\bar{B})$ where $P(\bar{A}$ and $\bar{B})$, the probability of receiving neither message is

$$\bar{P}(\infty)\ \bar{P}(p\Delta t)^{J}\ \bar{P}[(N-p)\Delta t)]^{J-1}$$

$$= e^{-M\tau e^{-(N-p)\Delta t/\tau}} \; e^{-M\tau J(1-e^{-p\Delta t/\tau})} \; e^{-M\tau J\,(1-e^{-(N-p)\Delta t/\tau})} \quad .$$

Since a broadcast time, t, = $JN\Delta t$, we see that

$$P\ (\bar{A} \text{ and } \bar{B}) = e^{-M\tau e^{-(N-p)\Delta t/\tau}} \; P_p \; P_{N-p}$$

where $\quad P_p = e^{-M\tau t}\left[1-e^{-p\Delta t/\tau}\right]/N\Delta t$

At this point, we will ignore the multiplying factor, $e^{M\tau e^{-(N-p)\Delta t/\tau}}$, since $M\tau \ll 1$ and for later simplicity in nomenclature

so $\quad P(\bar{A} \text{ and } \bar{B}) = P_p P_{N-p}$,
$\quad P(\bar{A} \text{ or } \bar{B}) = 2P_N - P_p P_{N-p}$, approximating $\bar{P}(J) = P_N$.

We then have for one message sent continuously with no spacing (N=1) the probability of receipt,

$$PMR = 1-P_1.$$

For two messages sent continuously with no spacing (N=2), the probability of receipt of both is

$$PMR = 1 - P(\bar{A} \text{ or } \bar{B}) = 1 - 2P_2 + P_1^2.$$

If three messages are sent in a packet $N\Delta t$ with separations of $(p-1)\Delta t$ and $(q-1)\Delta t$

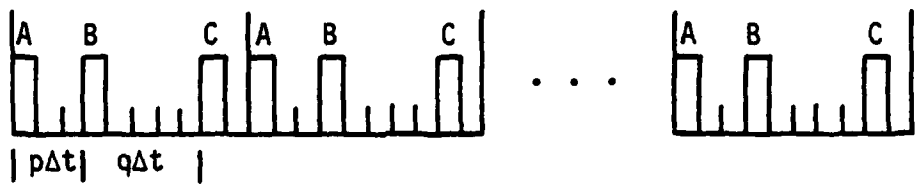

the probability of not receiving the three,

$P(\bar{A} \text{ or } \bar{B} \text{ or } \bar{C}) = P(\bar{A} \text{ or } \bar{B}) + P(\bar{C}) - P([\bar{A} \text{ or } \bar{B}] \text{ and } \bar{C})$

Since $P(\bar{A} \text{ or } \bar{B}) = P(\bar{A}) + P(\bar{B}) - P(\bar{A} \text{ and } \bar{B})$,

$P([\bar{A} \text{ or } \bar{B}] \text{ and } \bar{C}) = P(\bar{A} \text{ and } \bar{C}) + P(\bar{B} \text{ and } \bar{C}) - P(\bar{A} \text{ and } \bar{B} \text{ and } \bar{C})$,

$$P(\bar{A} \text{ or } \bar{B} \text{ or } \bar{C}) = P(\bar{A}) + P(\bar{B}) + P(\bar{C}) - P(\bar{A} \text{ and } \bar{B}) - P(\bar{A} \text{ and } \bar{C}) - P(\bar{B} \text{ and } \bar{C}) + P(\bar{A} \text{ and } \bar{B} \text{ and } \bar{C})$$

$$= 3P_N - P_p P_{N-p} - P_{p+q} P_{N-p-q} - P_q P_{N-q} + P_p P_q P_{N-p-q}$$

If the three are sent continuously with no spacing (N=3), the probability of receiving all three

$$PMR = 1 - 3P_3 + 3P_1P_2 - P_1^3 \quad .$$

Continuing the analysis to N messages,

$$PMR = 1 - NP_n + \Sigma P(\bar{A}_1 \text{ and } \bar{A}_2) - \Sigma P(\bar{A}_1 \text{ and } \bar{A}_2 \text{ and } \bar{A}_3) + \ldots + (-1)^m \Sigma P(\bar{A}_1 \text{ and } \bar{A}_2 \text{ and } \ldots \text{ and } \bar{A}_m) \ldots + (-1)^N P_1^N$$

where $\Sigma P(\bar{A}_1 \text{ and } \bar{A}_2 \text{ and } \ldots \text{ and } \bar{A}_m)$ is the sum over all combinations of m messages in N slots of the probabilities of the combination not being received.

For N = 4

$\Sigma P(\bar{A}_1 \text{ and } \bar{A}_2) = 4P_1P_3$ for the combinations

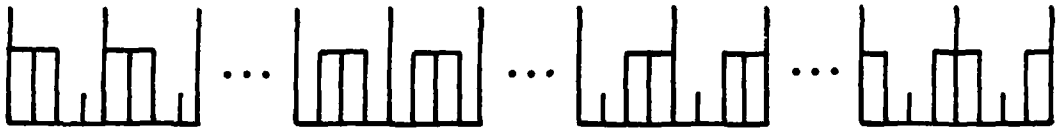

plus $2P_2^2$ for the combinations

Similarly $\Sigma P(\bar{A}_1 \text{ and } \bar{A}_2 \text{ and } \bar{A}_3) = 4P_1^2P_2$ for the combinations

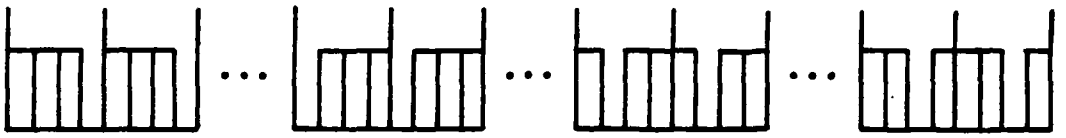

so $$P(4) = 1-4P_4 + 4P_1P_3 + 2P_2^2 - 4P_1^2P_2 + P_1^4.$$

The next four formulas of PMR are

$$N=5,\ PMR = 1 - 5P_5 + 5P_1P_4 + 5P_2P_3 - 5P_1^2P_3 - 5P_1P_2^2 + 5P_1^3P_2 - P_1^5 ,$$

$$N=6,\ PMR = 1 - 6P_6 + 6P_1P_5 + 6P_2P_4 + 3P_3^2 - 6P_1^2P_4 - 12P_1P_2P_3 - 2P_2^3 + 6P_1^3P_3 + 9P_1^2P_2^2 - 6P_1^4P_2 + P_1^6 ,$$

$$N=7,\ PMR = 1 - 7P_7 + 7P_1P_6 + 7P_2P_5 + 7P_3P_4 - 7P_1^2P_5 - 14P_1P_2P_4 - 7P_1P_3^2 - 7P_2^2P_3 + 7P_1^3P_4 + 21P_1^2P_2P_3 + 7P_1P_2^3 - 7P_1^4P_3 - 14P_1^3P_2^2 + 7P_1^5P_2 - P_1^7 ,$$

$$N=8,\ PMR = 1 - 8P_8 + 8P_7P_1 + 8P_6P_2 + 8P_5P_3 + 4P_4^2 - 8P_6P_1^2 - 16P_5P_2P_1 - 16P_4P_3P_1 - 8P_4P_2^2 - 8P_3^2P_2 + 8P_5P_1^3 + 24P_4P_2P_1^2 + 12P_3^2P_1^2 + 24P_3P_2^2P_1 + 2P_2^4 - 8P_4P_1^4 - 32P_3P_2P_1^3 - 16P_2^3P_1^2 + 8P_3P_1^5 + 20P_2^2P_1^4 - 8P_2P_1^6 + P_1^8 .$$

Finally, in the event that more than one relay is transmitting an N packet message, the PMR increases not only because of multiple chances to receive the whole message but also the possibility of receiving some packets from one relay and the rest from other relays. As before, the PMR is given in terms of sums of probabilities

$$P(\bar{A}_1 \text{ and } \bar{A}_2 \text{ and } \ldots \text{ and } \bar{A}_m) = \prod_j P_j$$

where the values of j in the product depend on the positions of the packets in the N packet message. For L relays transmitting this becomes

$$\prod_{i=1}^{L} \prod_j P_j(i) = \prod_j \prod_{i=1}^{L} P_j(i).$$

The PMR is thus calculated as before for one link with the sole change being P_j replaced by

$$\prod_{i=1}^{L} P_j(i) \quad \text{where } P_j(i) \text{ is calculated for the ith link.}$$

REFERENCES

1. Final Report, "Analysis of Meteor Burst Communications for Navy Strategic Applications," for Naval Ocean Systems Center, Contract No. N66001-79-C-0460, February 4, 1980.

2. Heritage, J.L., J.E. Bickel, and C.P. Kugel, "Meteor Burst Communication in Minimum Essential Emergency Communication Network (MEECN)" for the Defense Communications Agency (DCA), Command and Control Technical Center (CCTC), August 16, 1977

3. Sugar, George, R., "Radio Propagation by Reflection from Meteor Trails," ProcIEEE, v52, 2, p116-137, February 1964.

4. Oetting, John, "Analysis of Meteor Burst Communications for Military Applications," IEEE Trans. Commun., Vol. COM-28, September 1980.

APPENDIX B
IMPLEMENTATION

The implementation of the overdense formulas into the VHF(MB) Link Performance Model requires the redefinition of repeated quantities for minimum running time. For the same reason the flow diagram will appear repetitious. For example, the overdense formulas are shown separately for the cases $q_1=1$ and $q_1>1$.

For the $q_1=1$ case we require

$\overline{P_o}\ (T-t_o,\ \Delta t+t_o)$ in which case our defined

$$B \equiv \frac{\Delta t}{q_1\tau} = \frac{\Delta t+t_o}{\tau} = -\ \ell n\ S_o$$ from the definition of t_o and the fact that

Δt is $\Delta t+t_o$ for this case. In the definition of $A \equiv \frac{T+\Delta t}{q_T\tau}$, the sum, $T+\Delta t$, is unchanged. We define $D \equiv \Delta t/\tau$ so that $q_o = e^{D-B}$ so the first check on underdense or overdense is $D \geq B$ in the flow chart on Figure B-1.

Because the formulas will be used for the special cases $T = P\Delta t$, $1 \leq P \leq N$; we define $TT = (P+1)D$ so $A = TT/q_T$. In the underdense case $D<B$, the check to see if overdense formulas are not also required, $t_o \geq T$, becomes $B \geq TT$ by substitution. If the check is positive, the underdense formula of reference 1 is used. This is

$$\overline{P_u} = e^{-M_o\tau\ \frac{t}{N\Delta t}\ Q_p}$$

where $Q_p = (1-e^{-T/\tau})/q_o$. The term $\frac{t}{N\Delta t}$ is the multiplier of the probability of no useful meteor trail for $\frac{t}{N\Delta t}$ repetitions where t is the broadcast time. Since the quantity that differentiates the various situations is Q_p, this is calculated first.

If the check is negative, the fact that the probability is the product of

$$\overline{P_u} = e^{-M_o\tau\ \frac{t}{N\Delta t}\ (1-q_o)/q_o}$$

and the overdense $\overline{P_o}$ is accounted for by adding $1/q_o-1$ to the Q_p calculated for $\overline{P_o}$.

In this case the check for the situation of Figure 4 or 5 which is $\frac{\Delta t}{\tau} \geq q_2$ becomes $B \geq q_2$. If negative, the situation of Figure 4 applies. The next check $\frac{T+\Delta t}{\tau} \leq q_2$ is written $TT \leq q_2$. If positive we must obtain q_T from the transcendental equation

$$q_T = S_o^4 \, e^{4(T+\Delta t)/(\tau q_T)}$$

which in this case is $q_T = e^{4(A-B)} = e^{4\left(\frac{TT}{q_T} - B\right)}$. The first time this is encountered, the solution should be near unity so q_T is initialized at unity. For subsequent entries at higher values of P, the previously obtained q_T initializes the next search for the solution.

For $TT > q_2$, we have entered the situation of Figure 5 and must obtain the quantity q_M from the transcendental equation

$$q_M = q_2 e^{4(TT-q_M)} \quad .$$

Since $q_M = q_2$ at the check point $TT = q_2$ we initialize q_M at q_2.

For $B \geq q_2$, we are in the situation of Figure 5 from the beginning. The integration is between $q_3 = 1$ and the q_M found as before.

For $q_o \geq 1$, we have the overdense case. If $D < q_2$, we must redefine $BB \equiv (\Delta t/q_1\tau) = (D/q_1)$ where q_1 must be obtained from the transcendental equation

$$q_1 = e^{4(BB-B)} \quad .$$

We use q_o as the initial guess. We then do the check $TT \leq q_2$. If positive, we find $A = TT/q_T$ from the same equation as before but this time the initial guess can not be $q_T = 1$ since we know $q_1 \leq q_T \leq q_2$. We start the search at $q_T = q_1$ and start subsequent searches at the previously obtained q_T. For $TT > q_2$ we obtain q_M as before.

For $D \geq q_2$ we must find the starting value q_3 from the equation

$$q_3 = q_2 e^{4(D-q_3)}$$

where we use $q_3 = q_2$ for the initial guess.

Upon obtaining the appropriate values of Q_p, we generate the

$$P_p = e^{-M_o \left[\frac{t}{ND}\right] Q_p}$$

which replaces the formula on page A-12 of reference 1 (Appendix A). All further formulas to obtain the probability of message receipt, PMR, are unchanged.

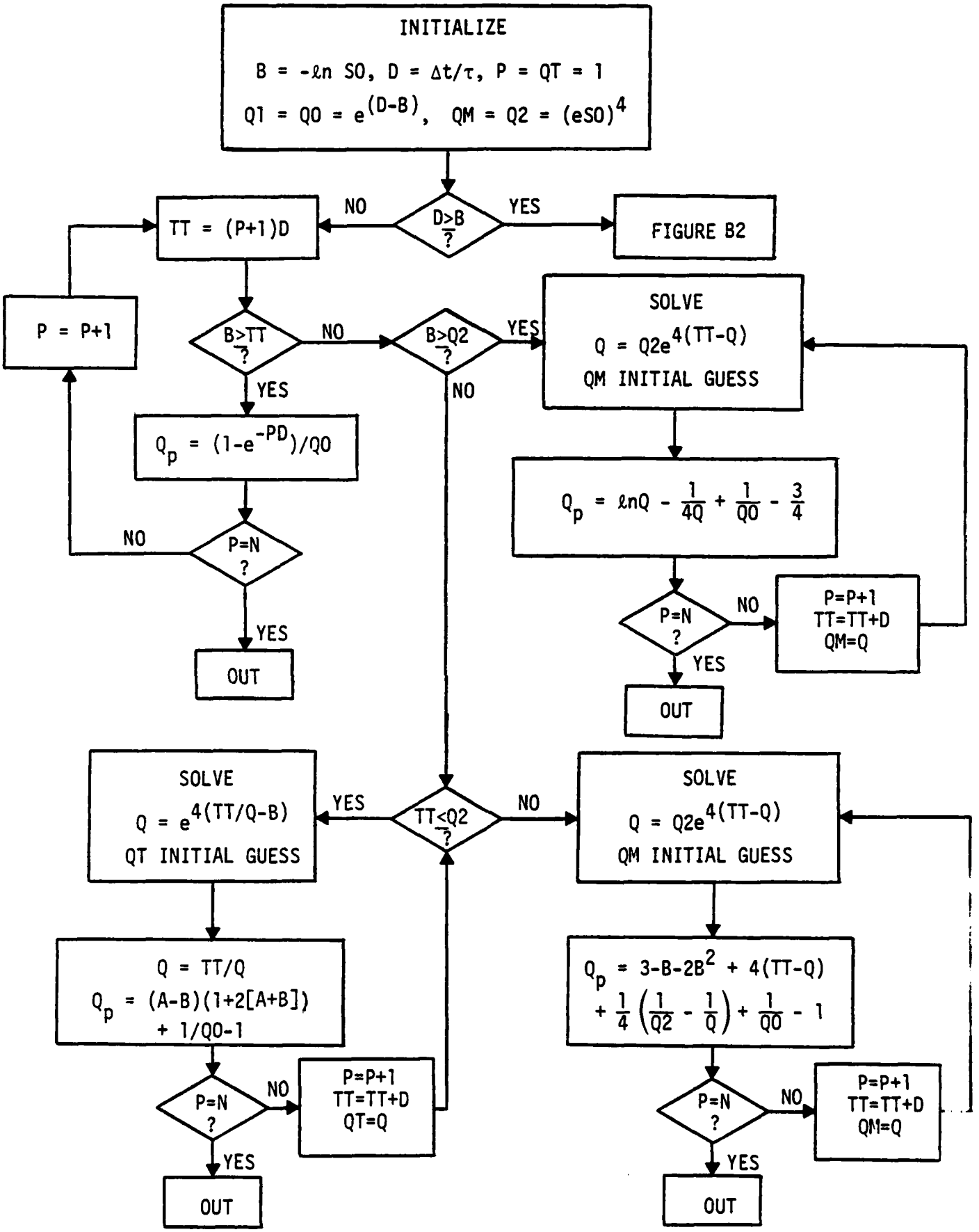

Figure B1. Program Flow Chart, Underdense.

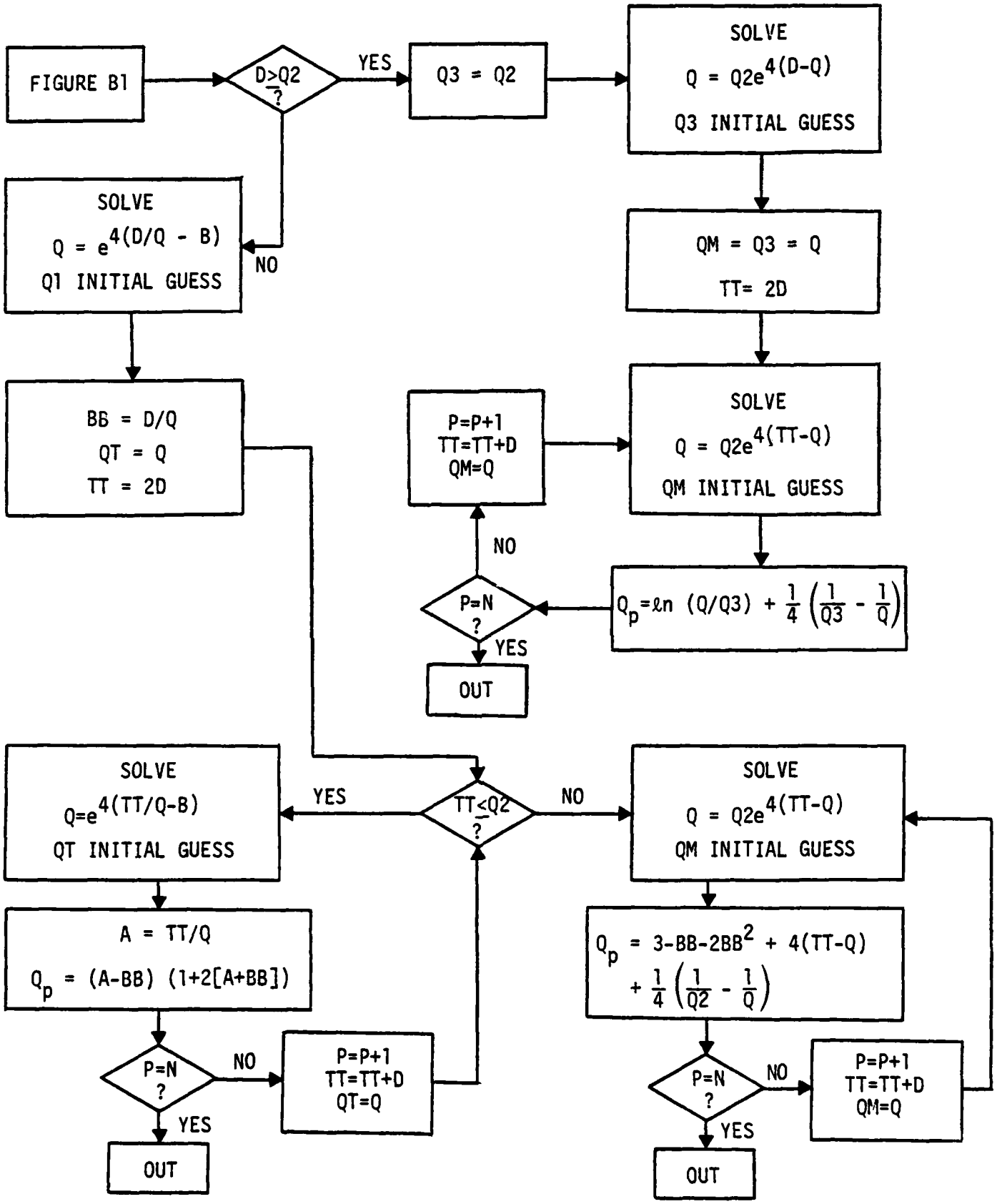

Figure B2. Program Flow Chart, Overdense.

END

FILMED

3-85

DTIC